Computers, Environment and Urban Systems 128 (2026) 102440

Contents lists available at ScienceDirect

Computers, Environment and Urban Systems

journal homepage: www.elsevier.com/locate/ceus

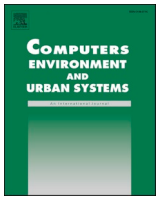

Urban housing markets under flood risk: Modeling demand pressure, risk perception bias, and public interventions

Asli Mutlu *, Tatiana Filatova *

Department of Multi-Actor Systems, Faculty of Technology, Policy and Management, Delft University of Technology, Delft, the Netherlands

ARTICLE INFO

Keywords:
Housing markets
Agent-based modeling
Flood risk perception
Nature-based solutions

ABSTRACT

Urban housing markets increasingly face escalating flood risk alongside persistent scarcity and affordability constraints. While these pressures shape price dynamics, their effects depend critically on heterogeneity in household risk perceptions and preferences. This study develops a spatial agent-based model (ABM) to examine how price differentials and residential patterns emerge from bottom-up interactions in a flood-prone urban environment. Parameterised to represent a typical city in the Netherlands, the model conducts scenario experiments that vary (i) market demand pressure, (ii) spatially heterogeneous individual risk perception biases, and (iii) public flood defense systems, including traditional defenses and nature-based flood defenses with co-benefits. Results show that market pressure and biased risk perceptions are the primary drivers of price growth and income-based exclusion, emerging well before flood defenses are introduced. Traditional flood defenses narrow flood-related price discounts by reducing objective risk, with nature-based defenses further reinforcing existing patterns through amenity capitalization. In both cases, public flood protection mainly reallocate demand spatially without altering overall market participation or affordability.

1. Introduction

Modern urban systems are increasingly shaped by the joint pressures of escalating climate hazards, persistent housing scarcity, and rising inequality (Glaeser & Gyourko, 2018; UN-Habitat, 2024). Worldwide, floods remain the costliest hazard (UNDRR and CRED, 2020), a concern that is intensifying as rapid urbanization spreads along rivers and coasts (Aerts et al., 2014; Hallegatte et al., 2013; IPCC, 2022). To manage flood risk, governments commonly deploy public flood protection measures. Yet these interventions do not occur in isolation: instead, they often add a layer of complexity to already strained housing markets. Traditionally, such public interventions are evaluated on engineering or ecological performance, including reduced hazard probability, avoided damage, or enhanced ecosystem services, while overlooking their effects on the socio-economic consequences of housing market dynamics. By changing both objective safety and the perceived desirability of locations, public flood protection can shift housing demand, alter price formation, and redefine who can afford to live in protected or amenity-rich neighborhoods (Anguelovski et al., 2022; Bockarjova et al., 2020). These socio-economic feedbacks are central to understanding whether public interventions, including public climate change adaptation, reduce hazard exposure equitably, but they remain insufficiently reflected in quantitative assessments of policy outcomes (Engbersen et al., 2024; van Ginkel et al., 2025).

Public flood protection strategies, whether traditional infrastructure defenses (e.g., levees, dikes) or nature-based solutions (NbS) (e.g., restored wetlands, green corridors), are designed to reduce the objective probability and enhance long-term resilience. At the same time, they can influence how households perceive the safety and value across space. When private actors underestimate flood risk, such risks may not be adequately reflected in housing prices (Baldauf et al., 2020; Bernstein et al., 2019). This mispricing can inflate property values in climate-sensitive areas and increase financial vulnerability when households unknowingly take on more risk than the market efficiently reflects (Gourevitch et al., 2023). As climate impacts intensify and insurance becomes less affordable or unavailable, such mispriced properties may face abrupt revaluations and may even become stranded assets (Bank of England, 2021; van Reeken & Phlippen, 2022). These market responses can amplify inequality in hazard-prone areas, leading to climate gentrification (de Koning & Filatova, 2020; Taylor & Aalbers, 2022).

Analyzing these diverse market responses and the distributional impacts of risks and public interventions requires a framework that

* Corresponding authors.
E-mail addresses: a.mutlu@tudelft.nl (A. Mutlu), t.filatova@tudelft.nl (T. Filatova).

https://doi.org/10.1016/j.compenvurbsys.2026.102440
Received 15 September 2025; Received in revised form 13 February 2026; Accepted 7 April 2026
Available online 30 April 2026

integrates the spatial relocation of people and shifts in urban housing values. Housing markets in flood-prone cities could respond to hazards, or changes in their probabilities due to public interventions, by pricing safe and exposed properties differently. Besides assessing aggregated structural shifts in markets, we are also interested in how these dynamics reshape inequality across locations and income groups. In this study, we focus primarily on changes in the spatial allocation of housing demand across safe and flood-prone areas, and on the distributional implications that emerge through price capitalization, exclusion, and changing access to protected or amenity-enhanced locations (Guerrieri et al., 2013). Public interventions may therefore alter where demand concentrates and who can access protected or amenity-enhanced neighborhoods, with consequences for socio-spatial inequality.From a political economy perspective, public investment can also generate uneven gains through capitalization, as collective risk reduction may increase private asset values and disproportionately benefit incumbent owners. These dynamics may produce unintended consequences, including increased population and asset concentration in hazard-prone areas associated with *the levee effect* (Di Baldassarre et al., 2015; Tobin, 1995), or 'climate gentrification' linked to financial change (Taylor & Aalbers, 2022) or 'greening' (Rice et al., 2020).

Notably, another critical driver shaping housing prices and inequality in hazard-prone cities is distorted individual risk perception. Insights from environmental psychology and behavioral economics show that individuals rarely evaluate low-probability, high-impact risks solely based on objective probabilities, but instead rely on simplified judgments, salient cues, and subjective interpretations of likelihood and consequences (Bubeck et al., 2012; Kahneman & Tversky, 1979; Robinson & Botzen, 2019). In housing markets, such biases may lead households with low risk perceptions to settle in hazard-prone neighborhoods, thereby artificially fueling prices that eventually fail to reflect actual risks (Filatova et al., 2011; Pryce et al., 2011). Empirical evidence further shows that flood risk perception varies substantially across households facing similar objective exposure, reflecting heterogeneity in how risk information is interpreted and internalized (Botzen et al., 2009a; Mol et al., 2020). While spatial salience and hazard visibility, such as proximity to rivers or flood zones, play a significant role in shaping perceived risk (Lechowska, 2018; O'Neill et al., 2016), these cues alone do not fully explain observed dispersion in subjective perceptions. In highly protected contexts, like the Netherlands, this heterogeneity in individual risk perceptions persists despite high information availability, underscoring that risk misperception is not reducible to information deficits alone.

These behavioral mechanisms are particularly relevant for nature-based flood protection, which combines risk reduction with visible environmental improvements. Unlike traditional defenses, NbS often generate recreational, aesthetic, and ecological co-benefits that increase neighborhood attractiveness and become capitalized into property values (Anguelovski et al., 2022; Bockarjova et al., 2020; Frantzeskaki, 2019; Seddon et al., 2020). While such benefits improve urban livability, they can also intensify competition for space in already constrained housing markets, raising concerns about social exclusion. Whether NbS reallocate demand or reinforce affordability pressures remains an open question with direct policy relevance.

In this context, the objective of this study is to assess how public hazard protection interacts with market dynamics and heterogeneous behaviors, here, biased individual risk perceptions, in urban environments. We quantify the cumulative and distributional consequences of these intertwined behavior–economy–hazard dynamics, focusing on housing prices, spatial allocation patterns, and income-based exclusion in flood-prone cities. Because the dynamics examined here emerge from heterogeneous subjective risk perceptions, decentralized and location-specific price adjustments, and feedback between individual location and price choices and aggregate market outcomes, they cannot be adequately captured by equilibrium or econometric models that rely on representative agents, complete information, or market-clearing assumptions. Agent-based modeling (ABM) is particularly suited to this research, as it allows heterogeneous household decisions shaped by bounded rationality and subjective risk perception to interact with market institutions in a bottom-up manner, revealing emergent pricing and spatial allocation dynamics (Aerts, 2020; Axtell & Farmer, 2025; Taberna et al., 2020).

To this end, we employ an empirical spatial ABM of a flood-prone Dutch housing market to address three key research questions: (RQ1) What structural and behavioral mechanisms shape price formation in flood-prone housing markets? (RQ2) How do these dynamics influence housing affordability and income-based exclusion? and (RQ3) To what extent do traditional and nature-based public hazard protection strategies influence existing patterns and inequality? Our RHEA-NL model builds on the RHEA framework (Filatova, 2015). We adapt and extend the original model to reflect the Dutch housing-market conditions, flood-risk patterns, and heterogeneous household behavior, using empirical housing transition data. The model represents income-constrained household agents with heterogeneous risk perceptions, bidding strategies, and preferences for environmental amenities provided by NbS, as well as a realtor agent who updates price expectations based on simulated transactions. We simulate scenarios that vary market demand pressure, perceived flood risk, and public flood protection strategies, including traditional defenses and NbS. Such modeling enables us to combine mechanisms grounded in different theoretical traditions –urban economics focused on spatial allocation and access to location-specific advantages, political economy on inequality, and behavioral sciences on decisions under risk– to explore whether and when structural shifts in markets emerge, with corresponding distributional effects.

The remainder of the paper is structured as follows. Section 2 provides background on the study context and institutional setting. Section 3 outlines the empirical and behavioral basis of the RHEA-NL model and describes the scenario design. Section 4 presents results on price formation, sorting, and affordability across public flood protection strategies. Section 5 discusses key insights and policy implications. Section 6 concludes by reflecting on limitations and directions for future research.

2. Background

The Netherlands provides a particularly relevant context for examining the interaction between flood risk, housing-market pressure, public flood protection, and ongoing climate change adaptation. Over half of the population lives in flood-prone areas, while the housing system is among the most supply-constrained in Europe. Persistent demand, limited land availability, and strict planning regulations have contributed to long-term affordability pressures and rising inequality. These structural conditions create a highly complex environment, complicating how public interventions might influence the spatial distribution of households and price formation.

Dutch flood governance has a long history of engineered protection, but recent flood protection strategies have increasingly moved beyond purely defensive approaches. Programs such as *Room for the River* represent a fundamental shift in water management strategy by combining flood-risk reduction with spatial redesign and ecological restoration (OECD Environment Policy Papers, 2020; van Herk et al., 2015). Large-scale projects, including Grensmaas and Zandmaas, have reshaped river landscapes, created new natural areas, and enhanced recreational and aesthetic values.

At the same time, long-standing institutional flood protection has fostered high levels of public trust and relatively low perceived vulnerability. Empirical studies suggest that this institutional context is associated with systematic underestimation of residual flood risk, particularly in areas where visible protection measures signal safety (Botzen et al., 2009a; Mol et al., 2020). In combination with strong housing demand and limited supply, these characteristics shape the Dutch housing market context in which public flood risk management

policies are implemented.

3. Data and methodology

3.1. Model lineage and study area calibration

ABMs are well-suited to analyzing housing-market dynamics when policy interventions generate feedback between individual decision-making and market-level outcomes. This is especially relevant in settings where heterogeneous households form bids under bounded rationality, subjective risk perceptions, preferences for amenities, and income constraints, and where prices emerge endogenously through market interactions rather than being imposed as equilibrium outcomes (Arthur, 2021; O'Sullivan et al., 2016). By integrating spatial data with agent-level decision rules, ABMs can represent the complex, self-organizing dynamics of cities in which human behavior is fundamentally shaped by urban geometry, neighborhood context, and heterogeneous hazard exposure (Crooks et al., 2018). In such spatially explicit models, socio-spatial phenomena such as residential sorting, neighborhood filtering, and segregation emerge from households navigating landscapes characterized by localized amenities and environmental risks (Ettema, 2011; Magliocca et al., 2011).

Within these environments, the uneven spatial distribution of flood risk acts as a dynamic constraint on household location choices, shaping how perceived safety, affordability, and access to amenities jointly influence residential mobility. As a result, market-wide patterns of housing wealth inequality or displacement can emerge endogenously from localized interactions between household preferences, risk perceptions, and geographic context (Ge, 2017; Guerrero, 2020; Magliocca & Walls, 2018). In the context of public interventions, the ABM framework therefore allows us to examine how public protection interacts with market pressure and behavioral responses over time, producing feedback between price formation, residential sorting, and affordability that is difficult to capture using reduced-form econometric or equilibrium models.

Calibration focuses on representing a typical urban region in the Limburg province, where initiatives such as the Room for the River program have combined flood risk reduction with ecological restoration and spatial redesign. Rather than replicating a single municipality, RHEA-NL draws on empirical patterns in Dutch urban development and riverine public flood risk management to inform its structure and parameters. These include institutional flood protection norms, spatially concentrated risk exposure, and high demand for limited housing supply.

We initialize the model with 3000 residential properties, of which 30% are located in flood-prone zones. The synthetic housing stock is generated using a Gaussian density–based sampler trained on house transactions in Maastricht, the province's largest city and central transaction hub. This approach helps us produce price gradients consistent with those in Dutch cities while mitigating identification problems arising from low transaction volumes in exposed areas that could destabilize the adaptive rolling hedonic regression. The approach also enables forward-looking scenario analysis by varying exposure levels in line with urban expansion and climate change.

Our analysis of the housing stock indicates that approximately 35% of residential properties are located in protected flood-prone areas, while only 25% of empirical transactions occur in these zones (see Appendix A.1). This underscores the underrepresentation of exposed dwellings in market data. Setting the baseline flood-prone share at 30% therefore provides a conservative and balanced calibration that reflects both physical and market participation. Validation of the synthetic stock against empirical transactions is provided in Appendix A.2. Importantly, by working with a synthetic landscape, we avoid sensitivities associated with identifying individual properties that could otherwise be flagged as potential stranded assets.

3.2. Data and model parameters

The model integrates three data layers: geocoded empirical transaction data, geospatial flood information, and literature-based calibration values. Table 1 summarizes the data sources that form the empirical basis of RHEA-NL. Table 2 summarizes global, household- and property-level model parameters and sources.

3.3. Agents and states

Three entities interact. *Households* are heterogeneous in income (quintiles),[1] housing-expenditure shares, perceived flood risk, amenity taste, intended residence time, and responsiveness to failed trading attempts. At any given timestep, a household may be a seller, a buyer, or an inactive homeowner. Sellers are selected from inactive homeowners probabilistically based on residence duration; buyers arrive in proportion to sellers, with a scenario-specific (Table 3) demand multiplier that mimics scarcity pressure. Housing expenditure shares vary by income group, with low-income households allocating a larger share of income to housing costs, reflecting financial vulnerability. Buyers sample from a set of attractive listings with probabilities proportional to their expected utility rather than rigidly choosing the single highest-utility property. This probabilistic choice ensures that slightly less utility listings still receive offers, preventing overconcentration of bids and more accurately reflecting real-world trade-offs under bounded rationality. Each bid is scaled based on the relative expected utility of each property, with the most favored property receiving the most competitive offer. Sellers evaluate offers in descending order and typically aim to sell to the highest bidder. However, if the highest bidder withdraws, sellers can proceed with the next-best offer, thereby reducing transaction failures and avoiding unnecessary delays in property sales.

A *Realtor* agent forms price expectations for each property based on recent simulated transactions. *Properties* carry structural and locational attributes, a flood-prone indicator, objective flood probabilities, and distances to the river and to nature-based interventions.

Table 1
Datasets creating the empirical basis of RHEA-NL.

Data	Role in model	Source
House transactions (1995–2020)	Transaction prices and structural and locational property attributes are used to calibrate housing stock characteristics and initialize baseline house prices	NVM; Mutlu et al. (2023)
Inundation maps (1993–1995)	Historical delineation of flood-prone areas, used for validation of calibration	Rijkswaterstaat
Flood-prone areas (2025)	Current delineation of flood-prone and protected zones, used for calibration and exposure validation	Deltares
River and CBD coordinates	Reference points for Euclidean distance calculations to the CBD and river, used in hedonic and utility functions	OpenStreetMap

[1] Household incomes are initialized by anchoring purchasing power to the initial empirical housing price distribution to ensure that each income group can plausibly transact within its targeted price segment. Income remains fixed over a household's lifetime; the model does not represent income growth or mobility. During turnover, entering households are assigned incomes by resampling from the current simulated income distribution. Thus, changes in income composition over time reflect endogenous market sorting and entry–exit dynamics rather than individual income transitions.

Table 2
Description of model parameters.

Symbol	Description	Baseline / Distribution	Source
Global parameters			
FP^{obj}	Scenario-specific annual objective flood probability in flood-prone areas	1/50 (S1a-d); 1/250 (S2-S3)	Rijkswaterstaat
L	Flood damage ratio	= 0.17	Endendijk et al. (2023)
α_{NbS}	Maximum NbS amenity premium	= 0.02 (calibrated)*	Bockarjova et al. (2020)
β_{NbS}	Spatial decay rate of NbS amenity	≈ 0.002 (calibrated)*	Bockarjova et al. (2020)
γ	Strength of spatial salience bias	≈ 0.0007 per meter	Model design
ϕ	Strength of latent perception bias	≈ 1.70	Model design
λ	Strength of listing-time price discount	= 0.02	Model design
Household-level parameters (i: Household index)			
η_i	NbS amenity taste	Lognormal dist. ($\mu = 0$, $\sigma = 0.25$)	Bockarjova et al. (2020)
T_i	Intended residence time	Normal dist. ($\mu = 17$, $\sigma = 1.5$) years	Wigt et al. (2012)
b_i	Latent perception bias	Beta dist. ($\alpha = 3$, $\beta = 2$), ($\mathbb{E}[b] \approx 0.60$)	Model design
Property-level parameters (j: Property index)			
d_j	Distance to the river	Min, max: [8, 3700] meters, $\mathbb{E}[d] \approx 1500$ m	Own GIS analysis
δ_j	Number of steps remained unsold	Endogenous state variable	Model outcome
LT_j	Listing-time price discount (logarithmic, capped at $\bar{\delta} = 0.15$)	$= \min\{\bar{\delta}, \lambda\, ln(1+\delta_j)\}$	Model design

* Appendix A.3 provides the calibration details of NbS parameters.

3.4. Household decision rules

Buyers evaluate a subset of listings within their budget and assign an expected-utility valuation to each option. Consistent with bounded rationality, household agents do not solve a global constrained optimization problem; instead, they consider a limited choice set and select the highest-ranked affordable property. Utility is expressed in monetary units as an indirect certainty-equivalent measure, allowing households to compare alternatives under uncertainty based on individual risk perceptions and amenity preferences.

For household i considering property j, indirect utility is given by Eq. (1).

$$U_{ij} = P_j\left(1 + A_{ij} - E\left[L_{ij}\right] - LT_j\right). \quad (1)$$

P_j is the Seller's ask price, which is set based on the market valuation by the Realtor agent. Property-specific adjustments are applied to P_j: presence of NbS adds an amenity premium, A_{ij}, while expected flood losses, $E\left[L_{ij}\right]$, reduce expected value, U_{ij}. Properties that remain unsold face a listing-time discount, LT_j, reflecting urgency and competition among buyers. Heterogeneity representing individual preferences and biases is embedded in both the flood-loss and amenity components. The following subsections define each element in detail.

3.4.1. NbS amenity valuation

Nature-based solutions provide environmental co-benefits that households value heterogeneously. Amenity valuation decays with distance from the river:

$$A_{ij} = \alpha_{NbS}.\eta_i.e^{-\beta_{NbS}d_j} \quad (2)$$

where d_j a_{nbs} is the maximum amenity premium at the riverfront, η_i is a household-specific taste drawn from a lognormal distribution, β_{NbS} governs spatial decay rate given the distance of property j to the river (i.e., NbS project location), d_j. This specification ensures that NbS benefits are both spatially structured and heterogeneous across the population.

3.4.2. Flood risk, perception, and expected flood damage

3.4.2.1. Objective flood probability. Flood-prone properties face an annual objective flood probability, FP^{obj}, which varies by scenario (Table 3) but is held constant throughout each simulation. Scenarios without public protection (S1a-d) use $FP^{obj} = 1/50$, while public protection scenarios (S2 and S3) apply $FP^{obj} = 1/250$, consistent with Limburg's post-1993/1995 floods protection standards.

For household i planning to reside in property j for T_i years, cumulative objective probability of experiencing at least one flood is:

$$FP_{ij}^{obj} = 1 - \left(1 - FP^{obj}\right)^{T_i}. \quad (3)$$

3.4.2.2. Perceived flood probability. Households form subjective perceptions of flood risk that may differ from objective probabilities,

Table 3
Scenario configurations.

Scenario	Demand (Buyer/ Seller)	Flood Probability	Perceived Flood Risk Formation	Public Flood Protection	Purpose and relation to research questions
S1a	Low (1/1)	Uniform (1/50)	Objective	None	Establishes a baseline to isolate the effect of high flood risk in a non-competitive market (RQ1)
S1b	High (2/1)	Uniform (1/50)	Objective	None	Examines how scarcity alone drives affordability and prices (RQ1, RQ2)
S1c	High (2/1)	Spatially decaying (1/50)	Spatial salience bias	None	Investigates how simple distance-based heuristics shape buyer behavior RQ1, RQ2)
S1d	High (2/1)	Spatially decaying (1/50)	Spatial salience + latent perception biases	None	Represents a realistic Dutch market scenario with high demand and underestimated flood risk (RQ1, RQ2)
S2	High (2/1)	Spatially decaying (1/250)	Spatial salience + latent perception biases	Traditional defense	Assesses the impact of reduced flood risk with structural protection under misperceived risk (RQ1, RQ2, RQ3)
S3	High (2/1)	Spatially decaying (1/250)	Spatial salience + latent perception biases	NbS	Evaluates the combined effect of reduced flood risk and enhanced environmental amenities (RQ1, RQ2, RQ3)

depending on the scenario. In unbiased scenarios (S1a–b), households correctly perceive flood risk, such that perceived and objective probabilities coincide:

$$FP_{ij}^{\text{perc}} = FP_{ij}^{\text{obj}} \tag{4}$$

In biased scenarios (S1c–d, S2, S3), households distort objective flood risk through two behavioral components that capture salient spatial cues and unobserved heterogeneity in risk perception. The first component represents a spatial salience heuristic, whereby households infer lower flood risk when properties are located further from the river. In S1c, perceived flood probability is adjusted as:

$$logit\left(FP_{ij}^{\text{perc}}\right) = logit\left(FP_{ij}^{\text{obj}}\right) - \gamma d_j, \tag{5}$$

where d_j denotes the distance of property j to the river, and γ controls the strength of spatial decay in perceived flood risk.[2]

The second component captures *latent idiosyncratic perception bias*, reflecting unobserved heterogeneity in how households interpret and internalize flood risk beyond spatial cues, for example, related to institutional settings like public flood protection. In S1d, S2, and S3, perceived flood probability is:

$$logit\left(FP_{ij}^{\text{perc}}\right) = logit\left(FP_{ij}^{\text{obj}}\right) - \gamma d_j - \phi b_i. \tag{6}$$

Here, b_i is a household-specific latent perception bias drawn from a right-skewed Beta distribution, implying that most households systematically underestimate flood risk, consistent with empirical evidence for highly protected contexts such as the Netherlands (Botzen et al., 2009b; Mol et al., 2020). The parameter ϕ scales the influence of this latent perception component.[3]

The resulting perceived probability, FP_{ij}^{perc}, is obtained via the inverse-logit transformation and used to compute expected flood loss.[4]

$$E\left[L_{ij}\right] = FP_{ij}^{\text{perc}}.L.P_j, \tag{7}$$

where L denotes the flood damage ratio (i.e., the fraction of property value expected to be lost conditional on a flood event) and P_j is the property's ask price.[5]

3.5. Bidding and trade

Buyers form a portfolio of attractive listings (max. 5 properties) by sampling in proportion to discounted expected utility, $\widetilde{U_{ij}}$. Within this portfolio, bids are scaled so that the most attractive property receives the highest offer, while less attractive properties receive proportionally lower bids. The household budget constrains the maximum bid.

Sellers set asking prices, P_j, relative to the Realtor's estimated market value, MV_j. Therefore, $P_j = MV_j + \varepsilon_j$, with $\varepsilon_j \in [-0.05, 0.05]$. They rank incoming bids, accept the highest feasible one, and fall back to the next-best if necessary. Both buyers and sellers adapt strategies if they remain unsuccessful.

3.6. Realtor and adaptive price expectations

At initialization, the Realtor agent uses empirical transaction data to price heterogeneous properties. As the simulation proceeds, the Realtor agent updates price expectations using an adaptive rolling hedonic regression on recent simulated transactions to elicit how the market trend evolves with buyers' and sellers' preferences and perceptions. For clarity, we present the hedonic in a compact form:

$$log\left(P_{jt}^{\text{trans}}\right) = \beta_0 + \sum_{k=1}^{K} \beta_k X_{jk} + \varepsilon_{jt}, \tag{8}$$

where X_{jk} includes structural (e.g., house size, rooms), locational (e.g., distance to CBD, distance to river), and risk attributes (floodplain indicator).

The Realtor initially updates price expectations using a two-year window of recent transactions. During periods of thin trading, when the number of successful transactions is insufficient to reliably re-estimate coefficients, the window is endogenously expanded up to a maximum of five years. When market activity increases, the model reverts to shorter windows, ensuring that price expectations remain responsive to recent market conditions. The five-year cap prevents outdated information from dominating price expectations. Similar adaptive expectation and estimation strategies are commonly used in agent-based housing and land market models, where agents update price beliefs based on recent transaction histories under data constraints (Magliocca et al., 2011; Parker & Filatova, 2008). The same procedure is applied consistently across all scenarios.

Full hedonic regression results estimated on the empirical dataset, including OLS and spatial regression models, are reported in Appendix A.4. Realtor uses OLS rolling hedonic on simulated transactions; spatial regressions are used only in empirical benchmarking, not within-agent pricing.

3.7. Scenario configurations

We use six simulation scenarios to isolate the effects of demand pressure, objective risk, risk perception, and public protection (Table 3). Our ABM model follows a fixed sequence of processes within each step, as illustrated in Fig. 1. Each simulation consists of 60 timesteps, with each step representing 6 months,[6] resulting in a 30-year simulated period, that corresponds to the standard mortgage maturity in the Netherlands and reflects the long-term horizon over which households typically evaluate housing and flood-risk exposure. To account for stochastic variation from randomized agent interactions and market matching, each scenario is executed 100 times using independent Monte Carlo runs.

3.8. Sensitivity analysis

We conduct both global and local sensitivity analyses to assess how key outcomes respond to parameter uncertainty. Appendix B reports a global sensitivity analysis based on the Morris Elementary Effects method (Morris, 1991), indicating that demand pressure is the primary driver of aggregate price and income levels, while flood-risk and perception parameters more strongly shape spatial price and income differentials; NbS-related parameters mainly affect price magnitudes. Appendix C presents a local sensitivity analysis in which flood-risk

[2] We assume that perceived flood risk halves at a distance of 1000 m from the river due to visibility effects. Accordingly, the strength of spatial decay is calibrated as $\gamma = ln(2)/1000$.

[3] To balance the two distortion channels at the population level, the strength of socio- institutional bias is calibrated as $\phi = \gamma\,(\mathbb{E}[d]/\mathbb{E}[b])$, where $\mathbb{E}[d]$ denotes the mean distance to the river in the housing stock and $\mathbb{E}[b]$ is the mean of household-specific latent perception bias, b_i, distribution. *Substituting the calibrated values yields*, $\phi = (\ln(2)/1000)(0.60/1500) = 1.70$, as reported in Table 2. This calibration ensures that distance-based salience and latent perception bias contribute equally to average risk underestimation, while preserving household- and location-level heterogeneity.

[4] $FP_{ij}^{perc} = \frac{1}{1+e^{\left[-\left(logit\left(FP_{ij}^{obj}\right)-\gamma d_j-\phi b_i\right)\right]}}$

[5] The damage ratio $L = 0.17$ follows recent empirical estimates reported for residential flood damages in the study area and is used here as a fixed expected loss fraction, as reported in Table 2.

[6] In the early stages of the model development, we have tested monthly, quarterly, semiannual and annual time steps. The semiannual time step appeared to perform best in terms of having sufficient simulated transactions to update the Realtor agent price expectation.

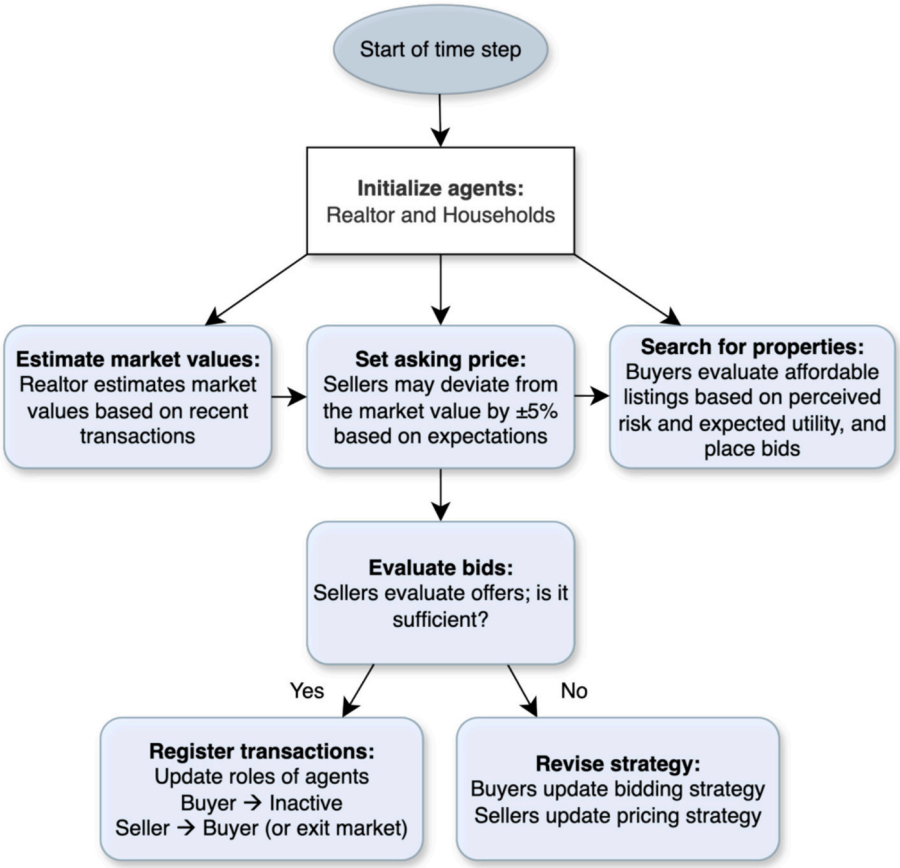

Fig. 1. Sequence of actions within one time step in the RHEA-NL agent-based housing market model.

perception bias intensity is varied by ±50% around the baseline calibration. More substantial bias reduces flood-prone price discounts and increases exposed asset values. In contrast, weaker bias produces the opposite effect, without altering the direction of price adjustments and spatial reallocation patterns. Together, these analyses indicate that the qualitative patterns reported in the Results section are not sensitive to small-to-moderate perturbations in key parameters.

4. Results

This section presents outcomes from the scenarios in Table 3. All reported results are based on averages across 100 independent Monte Carlo runs per scenario. The analysis proceeds sequentially: first establishing baseline patterns in housing price dynamics and spatial inequality under varying demand and perceived flood risk configurations (S1a-S1d), and then assessing how public flood protection strategies, such as traditional defenses and NbS (S2 and S3), modify these dynamics. Results are organized along four dimensions: (i) price formation and bidding behavior, (ii) aggregate exposure in flood-prone areas, (iii) income-based sorting and distributional outcomes, and (iv) spatial patterns of perceived flood risk.

4.1. Price formation and bidding behavior

4.1.1. Price dynamics for flood-prone and safe housing across scenarios

Transaction price dynamics across scenarios reveal how demand pressure, behavioral biases, and public protection cumulatively shape capitalization of flood risk (Fig. 2; Table 4).

In the baseline scenario (S1a), where demand is balanced and risk perception is objective, flood-prone properties sell for €235 k compared to €341 k in safe areas, reflecting a 30.9% discount. With supply roughly matching demand, buyers consistently internalize flood risk, maintaining a substantial price gap.

Under high demand pressure (S1b), intensified competition narrows the flood-prone discount to 24%, as constrained buyers bid more aggressively and risk sensitivity weakens. Introducing spatial salience in perceived flood risk (S1c) further compresses the discount to 15.4%, indicating that distance-based heuristics reduce capitalization of objective risk. When latent perception bias is added (S1d), the discount declines to 8.7%, as prices increasingly reflect perceived rather than objective exposure. This configuration (S1d), characterized by high demand pressure and systematic underestimation of flood risk, best approximates current Dutch urban housing conditions. The magnitude of the remaining discount is consistent with empirical hedonic estimates of our case study, which indicate a 7–12% discount for properties in flood-prone dike-ring areas,[7] depending on the regression specification (see Appendix A.4).

Public protection builds on these dynamics. Traditional defenses (S2) reduce objective flood probability and narrow the discount to 4.3%, while NbS (S3) nearly eliminate the gap (−0.4%) through combined risk reduction and amenity capitalization. Across scenarios, demand pressure and risk misperception account for the largest reductions in the flood-prone discount, with public protection contributing additional, but comparatively smaller, convergence.

Across scenarios, all price differences are statistically significant (p

[7] This gives us a compact external validity check against empirical data. However, in Table 4, we report unconditional mean differences in the final simulated year, whereas the regression coefficients are controlled effects from 1995 to 2020 data. Therefore, we do not aim to reproduce the exact same difference, only consistent sign and order-of-magnitude.

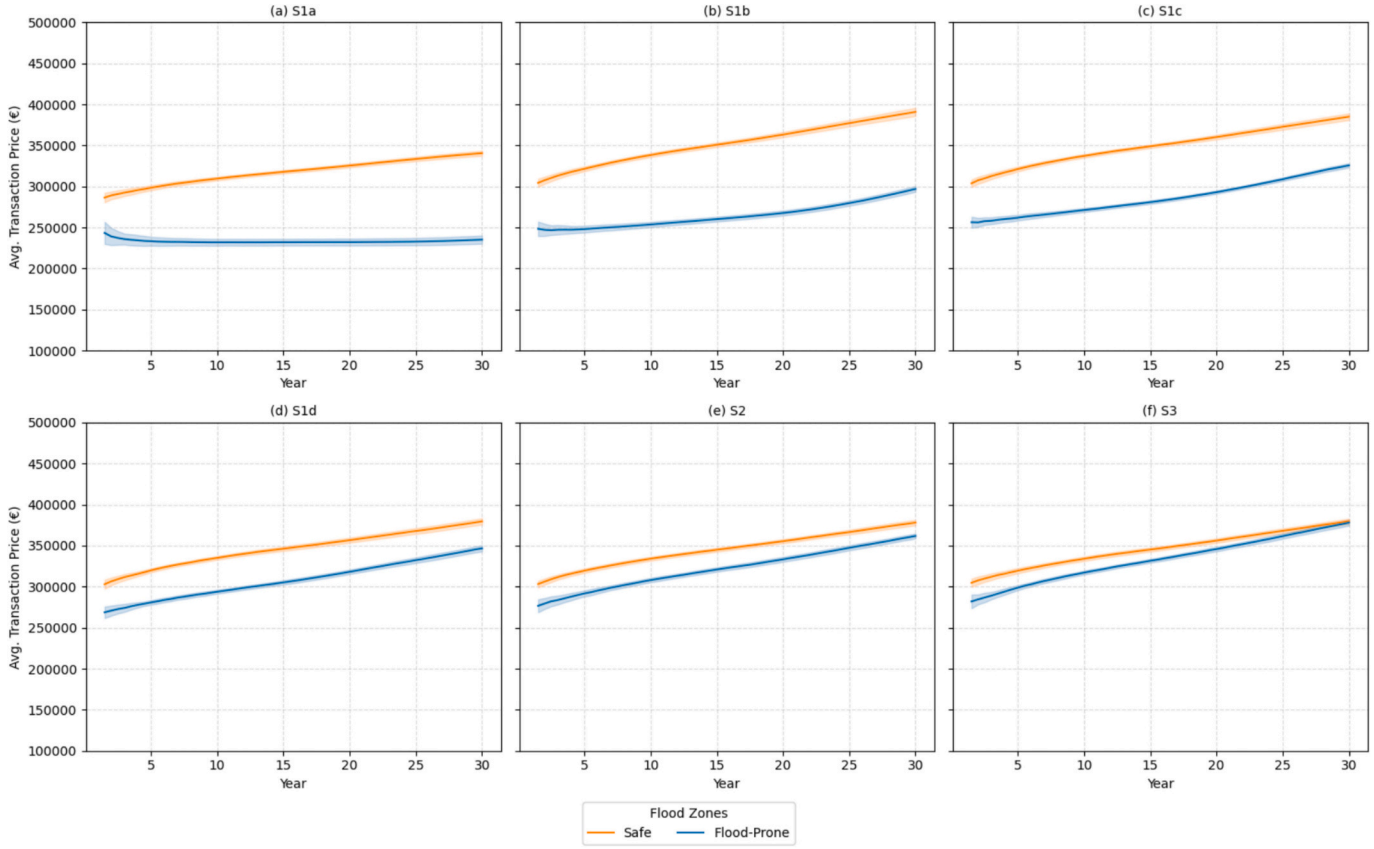

Fig. 2. Evolution of average transaction prices across scenarios in flood-prone and safe areas over time. Solid lines show mean transaction prices; shaded bands indicate the corresponding standard deviations (100 runs). Panels correspond to scenario variants: (a) S1a, a low-demand market with uniform objective flood risk (1:50); (b) S1b, high demand with unchanged objective risk; (c) S1c, where households infer lower flood risk with increasing distance from the river due to spatial salience; (d) S1d, which extends S1c by incorporating latent idiosyncratic perception bias; (e) S2, which applies traditional flood defenses to S1d, reducing flood probability to 1:250; and (f) S3, which builds on S1d by introducing nature-based solutions that both reduce flood risk and generate additional amenity value.

Table 4
Final-year housing prices and flood-risk discounts across scenarios.

Scenario	Price (€) (Market-wide)	Price (€) (Safe)	Price (€) (Flood-prone)	Price Discount (%) (Flood-prone vs. Safe)
S1a	306,158 (2196)	340,505 (3130)	235,190 (4967)	−30.9
S1b	361,907 (3915)	390,772 (4999)	296,909 (3494)	−24.0
S1c	366,968 (3348)	384,952 (4043)	325,602 (2596)	−15.4
S1d	369,639 (3645)	379,459 (3876)	346,568 (3815)	−8.7
S2	373,044 (3125)	377,925 (3350)	361,678 (3041)	−4.3
S3	379,100 (3098)	379,604 (3267)	377,936 (3784)	−0.4

Notes: Reported prices are mean transaction prices in euros at the final simulation year (Year 30). Standard deviations across 100 independent simulation runs are shown in parentheses. Market-wide prices combine transactions in safe and flood-prone areas. The price discount represents the percentage difference between mean prices in flood-prone and safe zones. Approximate marginal effects on the market-wide mean price are reported relative to the immediately preceding scenario: S1b (+18.21%), S1c (+1.40%), S1d (+0.73%), S2 (+0.92%), S3 (+1.62%), with S1a (€306,158) serving as the baseline.

< 0.001), reported in Appendix A.5. Together, these results show that hazard signals in prices progressively weaken as behavioral distortions and public interventions interact in competitive markets.

4.1.2. *Exposed asset values in flood-prone areas*

Changes in housing prices translate into substantial variation in aggregate exposure. We measure exposure using the Total Exposed Asset Value (TEAV), defined as the sum of property prices of all flood-prone properties at time t:

$$TEAV_t = \sum_{j \in \mathcal{F}} V_{j,t}, \tag{9}$$

where $V_{j,t}$ denotes the price of property j, and $\mathcal{F}$ is the set of flood-prone properties.

All scenarios begin with an identical baseline exposure of €245.36 million. By the final simulation year (Year 30), outcomes diverge markedly (Table 5). Under balanced demand and objective risk perception (S1a), TEAV declines to €214.97 million (−12%), reflecting limited buyer interest in risky locations. When demand pressure intensifies (S1b), TEAV rises to €267.15 million (+9%), despite unchanged objective risk. Introducing spatial salience and latent perception bias further amplifies exposure, increasing TEAV to €297.14 million (+21%) in S1c and €311.70 million (+27%) in S1d.

Public flood protection builds on these dynamics. Traditional defenses (S2) raise TEAV to €322.10 million (+31%), while NbS (S3) generate the highest exposure at €332.35 million (+35%). Because scenarios are constructed as nested counterfactuals that sequentially introduce market pressure, behavioral biases, and public protection strategies (Table 3), incremental changes in TEAV can be interpreted as marginal contributions of each mechanism (Table 5). The results indicate that most exposure growth occurs before public intervention, driven by intensified competition and risk misperceptions, while

Table 5
Final-year exposed asset values in flood-prone areas and incremental changes across scenarios.

Scenario	TEAV at Year 30 (€M)	Change from Year 0 (%)	Incremental Change (€M)
S1a	214.97 (0.03)	−12.39	–
S1b	267.15 (0.02)	8.88	+52.18
S1c	297.14 (0.02)	21.10	+29.99
S1d	311.70 (0.02)	27.03	+14.56
S2	322.10 (0.03)	31.27	+10.40
S3	332.35 (0.03)	35.45	+10.25

Notes: Total Exposed Asset Value (TEAV) is measured as the aggregate value of housing assets located in flood-prone areas at the final simulation year (Year 30), reported in million euros. Values in parentheses indicate standard deviations across 100 independent simulation runs. Percentage changes are cumulative relative to the baseline exposure in Year 0 (€245.36 million). Incremental Change reports the absolute difference in TEAV relative to the immediately preceding scenario, reflecting the marginal contribution of each sequentially introduced mechanism.

protection measures yield comparatively smaller incremental increases.

4.1.3. Bottom-up behavioral drivers of the housing price dynamics in hazard-prone areas

To examine the micro-level mechanisms underpinning the aggregate price and spatial allocation patterns observed across scenarios, we analyze household bidding behavior that emerges from the bilateral interactions of thousands of heterogeneous, boundedly rational traders. Specifically, we estimate scenario-specific OLS regressions on the model output data, using the bidding margin (i.e., the difference between the bid and asking prices) as the dependent variable. We focus on three key scenarios (S1d, S2, S3), all of which include heterogeneous flood risk perceptions. Table 6 summarizes the regression results, capturing how key household attributes, including income, affordability constraints (measured by the price-to-income ratio), and flood risk awareness, shape bidding behavior and market outcomes. Full regression results are provided in Appendix A.6.

Two consistent findings emerge. First, low-income households and those facing tighter affordability constraints bid more aggressively. Across all scenarios, log*(Income)* is negatively associated with the bidding margin ($p < 0.001$), while the price-to-income ratio (*Price/Income*) shows a strong positive relationship ($p < 0.001$). This suggests that economically constrained buyers are more likely to overbid to secure a property, especially in competitive or low-priced market segments. While this may seem counterintuitive, it reflects a deeper dynamic: riskier properties are often cheaper, and thus more accessible to low-income buyers. As these households face repeated rejection due to limited purchasing power, they gradually increase their bidding margins to remain competitive. However, since they are constrained by affordability thresholds (e.g., spending no more than 30% of their income on housing), this strategy requires shifting their search toward cheaper properties. Over time, this dynamic forces low-income households into lower-value, higher-risk housing, meaning they ultimately overpay relative to the objective flood risk of the properties.

Second, the relationship between objective flood probability (*Objective FP*) and bidding behavior is scenario-dependent and reveals a subtle but important shift under public flood protection. In the scenario without flood defenses (S1d), objective flood risk is moderately and positively associated with the bidding margin. This again reflects exclusionary pressures: high-risk areas are cheaper and thus attract constrained buyers. However, the coefficient becomes significantly larger in the public protection scenarios (S2 and S3), where objective risk is reduced from a 1-in-50 to a 1-in-250 flood probability. This pattern suggests that enhanced flood protection and environmental quality increase the appeal of formerly risky areas. These zones exhibit lower initial prices in the model because flood-prone properties are historically undervalued, as reflected in the empirical data used for calibration. Although prices evolve endogenously through agent interactions, these areas often remain more affordable than historically safer zones. Once public protection reduces objective risk, these areas, now safer yet still lower-priced, attract a wider pool of buyers. What may appear to be heightened risk tolerance is, in fact, a response to improved safety, affordability, and perceived opportunities in previously excluded locations.

Finally, the effect of risk perception bias (*RP bias*), the percentage difference between the objective and perceived flood risk, is modest across all three scenarios. While statistically significant in scenario S1d, its influence weakens under public protection and nearly disappears in S2 and S3. This suggests that while perceived flood risk may affect neighborhood selection or sorting, it plays a limited role in determining how much a buyer is willing to bid once a property has been chosen. In high-pressure housing markets, affordability and access constraints appear to dominate nuanced risk trade-offs.

Table 6
OLS regression results: determinants of bidding margins (dependent variable) across scenarios.

Variable	Coefficient (S1d)	Coefficient (S2)	Coefficient (S3)
log(Income)	−0.015***	−0.017***	−0.020***
Price/Income	0.142***	0.124***	0.093***
Objective FP	0.018***	0.083***	0.064***
RP Bias	−0.003***	0.000*	−0.001**

Note: Standard errors clustered by simulation run and household agent. Significance levels:*** $p < 0.01$, ** $p < 0.05$, * $p < 0.10$.

4.2. Distributional patterns across income groups and locations

We next examine how demand conditions, behavioral configurations, and public flood protection strategies influence the income composition of residents across flood-prone and safe areas (Table 7; Fig. 3). In this section, distributional change refers to shifts in the spatial distribution of income groups across locations, rather than to changes in household incomes themselves. Household incomes remain fixed over time; therefore, observed changes in mean income across zones reflect compositional shifts driven by market sorting and turnover, not changes in earning capacity.

Table 7
Final-year household incomes and income discounts across scenarios.

Scenario	Income (€) (Market-wide)	Income (€) (Safe)	Income (€) (Flood-prone)	Income Discount (%) (Flood-Prone vs. Safe)
S1a	50,911 (509)	58,820 (598)	34,566 (905)	−41.2
S1b	64,112 (901)	70,611 (1061)	49,479 (864)	−29.9
S1c	65,288 (685)	69,809 (780)	54,888 (629)	−21.4
S1d	65,981 (792)	68,688 (808)	59,621 (970)	−13.2
S2	66,601 (675)	67,981 (704)	63,388 (754)	−6.8
S3	66,893 (649)	67,116 (682)	66,381 (888)	−1.1

Notes: Reported values are mean annual household incomes in euros at the final simulation year (Year 30). Standard deviations across 100 independent simulation runs are shown in parentheses. Market-wide values combine households located in safe and flood-prone areas. The income discount represents the percentage difference between mean incomes in flood-prone and safe zones. Approximate marginal effects on mean market-wide income are computed sequentially relative to the immediately preceding scenario: S1b (+25.93%), S1c (+1.83%), S1d (+1.06%), S2 (+0.94%), S3 (+0.44%), with S1a (€50,911) as the baseline.

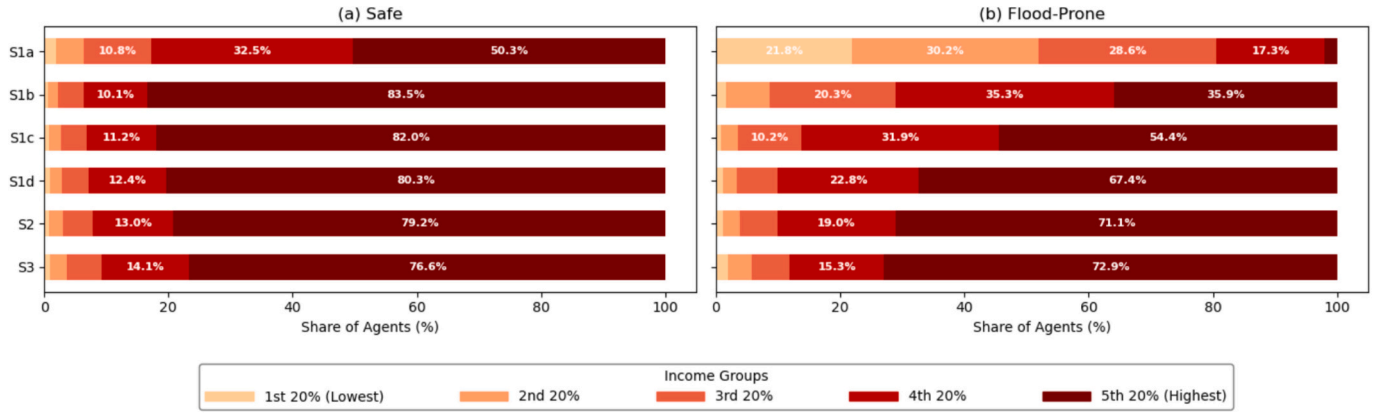

Fig. 3. Normalized income group composition in flood-prone and safe areas across scenarios at the final simulation year (Year 30), averaged over 100 simulation runs. Percentage shares above 10% are labeled directly on the bars for readability.

In the low-demand setting (S1a), participation is broadly feasible; however, households spatially sort according to affordability constraints. Low-income households disproportionately occupy flood-prone areas: over half of flood-prone residents belong to the bottom 40% of the income distribution (Fig. 3.b; S1a), and the mean household income is €34.6 k, 41.2% lower than in safe zones (Table 7). Even when overall affordability is maintained, market sorting produces socio-spatial inequality, as lower-income households concentrate in relatively cheaper, risk-prone areas.

Under intensified demand (S1b), exclusion becomes systemic. Increased competition for housing leads more individuals to overbid in an attempt to secure a home, thereby reducing affordability at the margins. Market-wide mean incomes rise to €64.1 k, while the share of the two lowest quintiles declines sharply in both zones (Fig. 3.b; S1b). In flood-prone areas, mean income increases to €49.5 k, narrowing the safe–flood-prone gap to 29.9% (Table 7).

Risk perception distortions further amplify spatial allocation patterns once demand pressure has already shaped market participation. From S1c to S1d, a downward bias in perceived flood probabilities reduces the risk premium on flood-prone properties. Under competitive bidding, however, higher-income households are better positioned to secure these increasingly attractive locations. Consequently, flood-prone areas attract a growing share of higher-income households (Fig. 3.b; S1c-S1d), while the safe zone correspondingly loses some of its high-income dominance (Fig. 3.a; S1c-S1d). Consistent with this mechanism, mean flood-prone incomes rise and the safe–flood-prone income gap narrows from 21.4% (S1c) to 13.2% (S1d) (Table 7).

The public intervention scenarios (S2-S3) inherit the behavioral flood risk perception and demand conditions from S1d. They therefore reflect the combined effects of risk misperception, housing scarcity, and objective improvements in safety and amenities within flood-prone areas. As a result, mean incomes in flood-prone areas rise further, narrowing the income gap with safe areas to 6.8% under traditional defenses (S2) and to 1.1% under NbS (S3) (Table 7). Fig. 3 (S2-S3) shows that this convergence is accompanied by a continued spatial reallocation of high-income households from safe to flood-prone areas. Notably, market-wide mean incomes change only marginally after S1c, indicating that public protection primarily reallocates demand rather than altering overall market participation.

4.3. *Spatial patterns of risk perception*

To explore the spatial consequences of behavioral biases and public flood protection strategies, we compare scenarios S1d, S2, and S3 using property-level heatmaps. Fig. 4 illustrates the distribution of individuals with subjective risk perception (RP) bias —defined as the deviation between perceived and objective flood risk—across space (Fig. 4.a-c).

In S1d (Fig. 4.a), the flood risk remains objectively high (1:50),

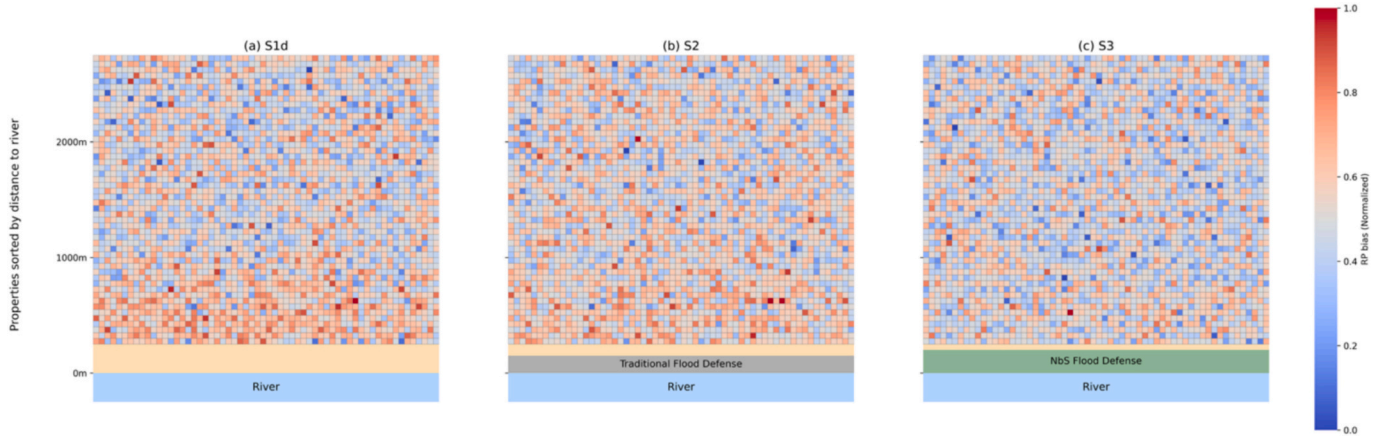

Fig. 4. Spatial distribution of combined risk perception bias (spatial salience and latent idiosyncratic perception bias) in three key scenarios: baseline with spatially decaying flood risk (S1d), traditional flood defense (S2), and nature-based solution (S3). Properties are ordered vertically by distance to the river (y-axis), while the horizontal dimension represents an abstract spatial index used for visualization rather than a geographic coordinate (x-axis). Panels a-c denote households with the highest individual risk perception bias in red color, and those who estimate the flood risks the most accurately with blue color. The results are the averages from the 100 independent runs of the RHEA-NL model. (For interpretation of the references to color in this figure legend, the reader is referred to the web version of this article.)

making spatial differences based on RP bias more salient. Here, behavioral biases play a larger role in household housing decisions: people who underestimate flood risk disproportionately settle near the river, where objective risk is highest. The resulting pattern—cluster of red shading under 1000 m distance band (Fig. 4.a) —indicates that buyers with distorted perceptions fail to internalize existing flood risk. Hence, they unknowingly expect high utility from those homes and overbid for them, artificially pushing demand for hazard-prone properties up. The pattern becomes more scattered when flood probability is reduced to 1:250 through traditional defenses in S2 (Fig. 4.b). While households with low-risk awareness still reside near the river, clustering is less pronounced. This shift reflects a reduction in the role of individual risk perception in shaping housing decisions, since objective risk and, thus, location-based safety cues, are diminished. In S3 (Fig. 4.c), when NbS offer the same level of protection as S2 but also add environmental amenities, the concentration of low-awareness households becomes more widespread throughout the space. This suggests that additional environmental benefits may further reduce households' risk sensitivity. Overall, spatial patterns associated with risk perception bias remain statistically different across all three scenarios ($p < 0.001$).

5. Discussion

This study investigates how public flood protection interacts with demand pressure and heterogeneous flood risk perceptions to shape housing prices, spatial allocation patterns, and distributional outcomes in a flood-prone urban housing market. The stepwise scenario design isolates the marginal contributions of demand intensity, behavioral distortions, and public protection strategies, allowing us to assess whether exclusionary outcomes stem primarily from adaptation measures or from pre-existing structural housing market conditions that characterize many urban regions.

5.1. Demand pressure, risk misperception, and market inequality

The results show that demand pressure is the primary driver of market-wide exclusion dynamics, while perceived flood risk distortions shape *where* households locate within the market once participation has already been filtered by affordability. Under low-demand conditions, lower-priced flood-prone areas remain relatively accessible to low-income households. As demand pressure increases, however, affordability becomes binding, and successful transactions become increasingly dominated by higher-income buyers, particularly in historically safer areas. This mechanism is consistent with empirical evidence from hazard-prone housing markets, where affordability constraints and competition for limited supply push vulnerable groups into lower-priced, higher-risk locations, contributing to patterns often described as climate gentrification (de Koning & Filatova, 2020; Kousky, 2010; Taylor & Aalbers, 2022).

Perceived flood risk distortions can further modify this demand-driven sorting. When households rely on spatial salience cues and exhibit latent perception bias, prices and bidding behavior increasingly reflect perceived rather than objective hazard exposure. In our model, these distortions reduce the flood-prone price discount and increase the attractiveness of river-adjacent locations for higher-income buyers. This is consistent with empirical findings showing incomplete capitalization of flood risk, particularly in contexts characterized by strong protective infrastructure or attenuated risk salience (Baldauf et al., 2020; Botzen et al., 2009a). More broadly, the results reinforce a key implication of behavioral and risk-perception research: even when information is available, households may rely on salient cues and subjective interpretations (Burningham et al., 2008; Mol et al., 2020), leading to heterogeneous valuations and market outcomes.

In the Dutch urban context, persistent housing shortages combined with relatively low flood risk salience may render climate risk a secondary sorting dimension once affordability constraints dominate participation (Groot & Groot, 2024). Importantly, our model does not attribute perceived risk distortions to specific institutional mechanisms (e.g., trust); instead, it captures reduced-form heterogeneity and systematic underestimation in perceived flood risk, consistent with survey evidence that perceived exposure varies across households facing similar objective conditions (Botzen et al., 2009a; Terpstra, 2011). A recent Dutch survey corroborates these findings, revealing that many Dutch households not only underestimate their individual flood risk but also tend to externalize responsibility to the state (Sirenko & Filatova, 2025). In our ABM, this combination of scarcity and perceived risk distortions contributes to the systematic underpricing of flood risk, reinforcing exposure patterns that are driven more by behavioral and institutional factors than by objective hazard risk alone.

5.2. Reallocative effects of public interventions

Public flood protection strategies build on top of these demand- and perception-driven dynamics. Both traditional defenses and NbS lower objective flood probabilities, and these improvements are capitalized in housing prices. Consequently, price differentials between flood-prone and historically safe areas narrow substantially, and the income gap between residents in these areas also compresses. At the same time, market-wide average income changes only marginally once demand pressure has already filtered market participation. This suggests that public protection does not transform who participates in the housing market, but primarily reshapes *where* higher-income households locate, reallocating demand from historically safer zones toward newly protected or amenity-enhanced floodplains.

These dynamics resonate with long-standing debates on the levee effect. Although structural protection reduces flood probabilities, it may also weaken hazard salience and encourage settlement in previously avoided areas (Tobin, 1995). A similar mechanism emerges in the model. Following the introduction of flood defenses, households' spatial sorting (Fig. 4.b) becomes less strongly patterned by perceived flood risk differences, not necessarily because households become more accurate, but because objective risk gradients are reduced and hazard salience weakens. In this sense, public defenses may unintentionally reinforce the very exposure they are designed to mitigate, a pattern widely observed in socio-hydrological literature (Baan & Klijn, 2004; Collenteur et al., 2015; Di Baldassarre et al., 2015).

NbS reinforce these existing patterns by coupling safety with environmental co-benefits. A growing body of international evidence suggests that the perceived value of NbS extends well beyond hazard reduction. Households often assign significant worth to the visual appeal, symbolic meaning, and everyday usability of green infrastructure, qualities that are usually capitalized into housing prices (Anguelovski et al., 2022; Bockarjova et al., 2020; Brander & Koetse, 2011; Frantzeskaki, 2019; Nesshöver et al., 2017; Votsis, 2017; Waltert & Schläpfer, 2010). While concerns about “green gentrification” are well documented (Anguelovski et al., 2019), our results offer a more nuanced perspective. In our results, NbS produce an additional convergence of prices and resident incomes between flood-prone and safe areas, though this incremental effect is modest relative to traditional defenses. Ultimately, the primary distributional implication is not a shift in market-wide affordability, but a strengthened spatial reallocation of high-income households toward protected flood-prone areas. This narrows cross-zone income differences while leaving underlying affordability crisis practically unchanged.

The convergence of prices and resident incomes across zones can be interpreted in two complementary ways. On the one hand, it indicates that markets recognize the benefits of public investment in risk reduction (and, for NbS, amenity enhancement). On the other hand, it implies that hazard signals embedded in price discounts weaken, potentially obscuring residual exposure and shifting risk-bearing toward households purchasing in newly protected locations. Which interpretation dominates depends on context, particularly the degree of residual risk,

the transparency and salience of risk information, and the affordability constraints faced by different income groups.

6. Conclusions

Rapid urban expansion and escalating climate-induced flood risk have intensified debates over how public interventions, including climate adaptation strategies, interact with social inequality in cities. Yet the mechanisms through which flood protection reshapes housing market outcomes remain insufficiently understood. Different theoretical traditions study various mechanisms in isolation: urban economics focuses on spatial sorting, political economy on inequality, and the behavioral sciences on decisions under risk. However, it is the interplay of these mechanisms that defines whether and when structural shifts in markets emerge, with corresponding distributional effects. This study examined how public flood protection interacts with housing market tightness and heterogeneous flood risk perceptions to shape property values at risk, spatial allocation patterns, and inequality outcomes in hazard-prone urban areas.

Using an empirically grounded agent-based model, we show that the dominant structural shift in market participation arises under high demand pressure. As competition intensifies, lower-income households are increasingly excluded from the market. Subjective flood risk perceptions further weaken the capitalization of objective flood risk into prices and reshape spatial allocation patterns by increasing the attractiveness of flood-prone areas. Yet these behavioral mechanisms operate within pre-existing structural market scarcity.

Within our stylized model of the Dutch market, our analysis shows that both NbS and traditional public flood interventions are capitalized into housing prices, narrowing price and income gaps between flood-prone and historically safe areas. However, once scarcity-driven exclusion is already in place, these interventions do not substantially alter who participates in the housing market. Instead, they shift demand toward newly protected and, in the case of NbS, amenity-enhanced floodplains, thereby increasing the value of properties in flood-prone areas while compressing cross-zone differentials. This finding contributes to a better understanding of how the famous 'levee effect' (Di Baldassarre et al., 2018) manifests across different market institutions. Previously, the 'levee effect' was shown to drive population and property value growth in another ABM analysis (Haer et al., 2020), which excludes market dynamics. Our results indicate that when such policy interventions interact with market mechanisms, especially in urban housing markets with space scarcity, the observed disparities between safe and newly enhanced hazard-prone areas, therefore, stem from persistent housing shortages, mispriced risk, and institutional market inefficiencies rather than from public intervention itself.

The magnitude and direction of these distributional effects depend on the interaction between public flood protection measures, housing market conditions, and the broader institutional setting. The *climate* gentrification created by the interplay of subjective risk perceptions and market forces in the context of the U.S. housing market (de Koning & Filatova, 2020) is not confirmed here, mainly because low-income households are already excluded from the market (either by experimenting with risk perceptions or public interventions in our model) before any flood-risk adjustments influence market outcomes. In the Dutch setting, strong public flood protection and high institutional trust may further reduce the salience of flood risk at the point of housing choice, particularly in a highly competitive market. In alternative market or institutional settings, where risk information is more salient or mediated through different governance and market instruments, the same behavioral mechanisms may interact with housing supply conditions and demand pressure to produce distinct distributional patterns. More broadly, the effects of public protection strategies cannot be understood independently of the behavioral and financial systems in which they operate. Whether traditional defenses or nature-based solutions, public risk management interventions interact with affordability constraints, price formation processes, and behavioral responses. Designing equitable adaptation strategies, therefore, requires explicit attention to these economic feedbacks (van Ginkel et al., 2025), particularly in high-demand urban settings where adaptation investments may otherwise reinforce existing inequalities and potentially trigger climate gentrification (Taylor & Aalbers, 2022).

This study makes a novel contribution by systematically unpacking how flood risk perception and urban housing markets interact with two public hazard interventions to shape socio-economic outcomes in cities. By complementing qualitative insights and empirical evidence in the housing and flood risk management literature, this work offers a quantitative perspective to understand how social disparities and risk exposure can emerge and evolve under different public protection strategies. However, our work is not without limitations. Future research could develop in several directions. First, incorporating institutional actors such as banks and developers would offer insights into how lending criteria, credit availability, or construction decisions influence access to safer housing. Second, exploring the role of market instruments, such as climate risk labels or disclosure mechanisms, could help evaluate their potential to promote transparency and correct distorted price signals in climate-exposed areas. Third, endogenizing income mobility and demographic change would be a valuable extension, allowing examination of longer-run social transformations beyond the spatial allocation patterns captured here. Lastly, while this study relies on empirically grounded but static flood damage estimates, future applications could allow both hazard intensity and vulnerability to evolve, for example, by linking damage ratios to depth-damage functions and changing exposure regimes. Exploring these complex dynamics under different climate change and population growth scenarios would further help bridge the gap between simulated dynamics and real-world decisions, offering insights for designing climate-resilient and socially just urban housing systems.

CRediT authorship contribution statement

Asli Mutlu: Writing – review & editing, Writing – original draft, Visualization, Validation, Software, Methodology, Investigation, Formal analysis, Data curation, Conceptualization, Updated software design. **Tatiana Filatova:** Writing – review & editing, Supervision, Project administration, Funding acquisition, Conceptualization, Original software design.

Acknowledgments

This work was supported by the Resilient Delta Initiative through the Converge grant, under the project *"Encouraging Climate Change Adaptation Through Climate Risk Labels"*, and by the Dutch Research Council (NWO) under the project *"Crossing Borders at the Grensmaas"* (grant number 17596). We thank NVM for providing house transaction data and Liz Verbeek for her assistance in converting the original RHEA model to Python. Tatiana Filatova also acknowledges support from the ERC SPHINX project (grant number 101171568).

Appendix A. Empirical grounding and model calibration

A.1. Spatial analysis of the residential stock and the empirical transaction data

Fig. A.1 contrasts the spatial distribution of the total residential housing stock in Maastricht with the subset of properties observed in empirical transaction data. While flood-prone areas, particularly those protected by public defenses, are well represented in the underlying housing stock, they appear less frequently in realized transactions. Fig. A.2 quantifies this discrepancy, showing that approximately 35% of residential dwellings are located in protected flood-prone areas, whereas only about 25% of observed transactions involve properties in these locations. This pattern indicates that flood-prone dwellings are systematically underrepresented in market data relative to their physical presence in the housing stock. Calibrating the baseline flood-prone share at 30% therefore provides a conservative and balanced representation that lies between physical exposure (stock) and realized market participation (transactions).

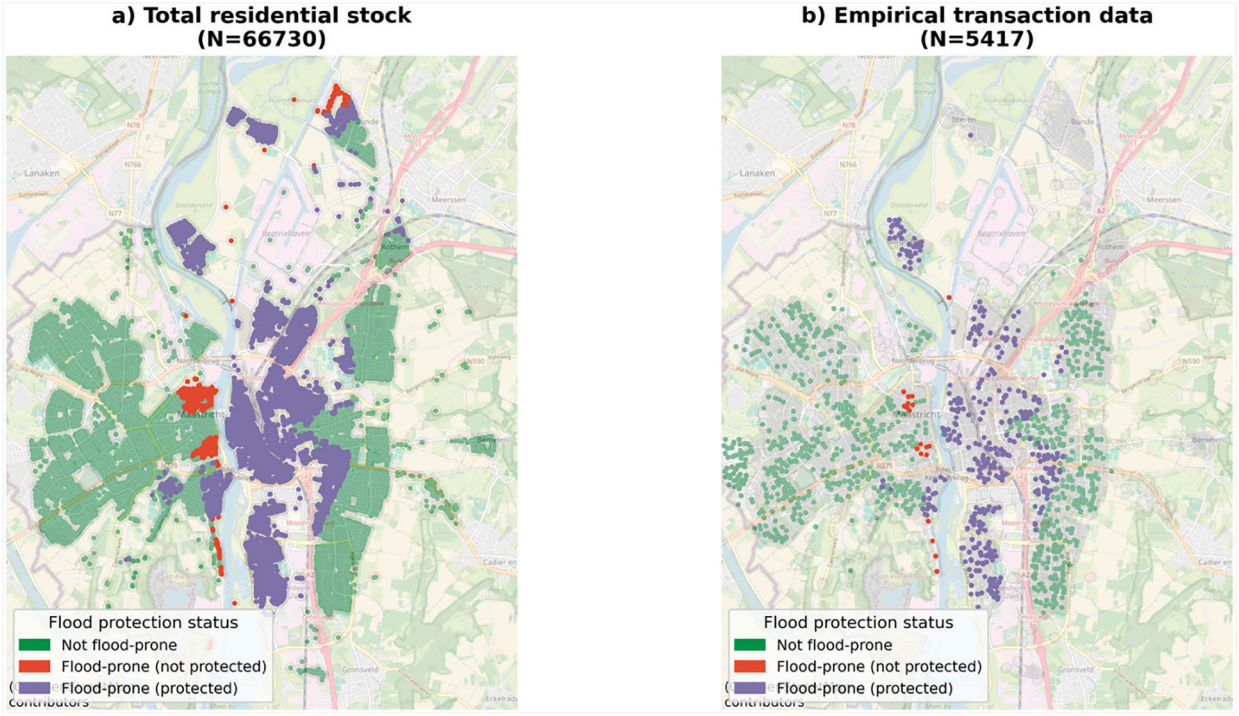

Fig. A.1. Spatial distribution of residential housing in Maastricht by flood-protection status: a) total residential stock from Dutch Land Registry (Basisregistratie Adressen en Gebouwen (BAG) in 2025, b) Empirical transaction data recorded by NVM realtors (1995–2020).

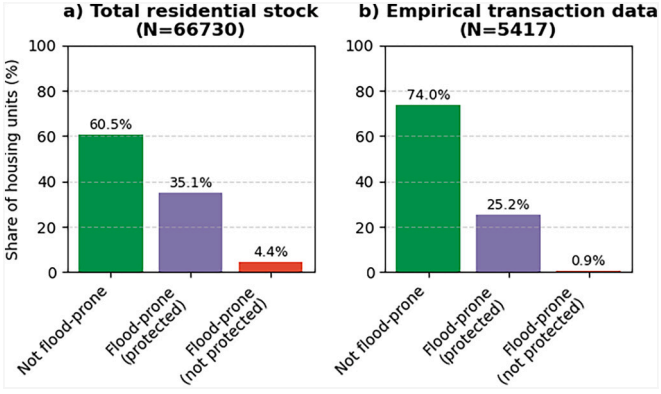

Fig. A.2. Percentage shares of residential housing in Maastricht illustrated in Fig. A.1. Note: Unprotected flood-prone properties are removed from the analysis due to limited data points.

A.2. Quantitative validation of the synthetic housing stock

This appendix provides quantitative validation of the synthetic housing stock used to initialize the agent-based housing market. We complement the visual comparisons in Fig. A.3 and Fig. A.4 with distributional distance and dependence metrics computed between the empirical housing transactions and the synthetic sample. Metrics are computed for key structural, locational, and price variables and are reported **separately for safe (FP = 0) and flood-prone (FP = 1) properties**, reflecting the stratified construction of the synthetic data.

A.2.1. Marginal distributions

Table A.1 reports Kolmogorov–Smirnov (K-S) distances and quantile-based RMSEs (1st–99th percentiles). Structural and locational attributes

(AGE_2020, HOUSESIZE, LOTSIZE, LN_DIST_CBD, LN_DIST_MEUSE) exhibit small K-S distances and close agreement across both strata, consistent with the ECDF overlaps in Fig. A.3. For log prices, the K-S test rejects equality due to large sample sizes, while quantile RMSEs and moments remain close, indicating preservation of price levels and dispersion.

A.2.2. Dependence structure

Fig. A.4 and Table A.1 assess rank dependence using Spearman correlations. The synthetic stock closely reproduces the empirical correlation structure, with low RMSE and MAE between correlation matrices in both flood-protection strata.

Table A.1
Stratified marginal distribution validation (K-S distance and quantile-based error).

FP	Variable	KS_D	KS *p*-value	Q_ RMSE	Q_ MAE	Emp. mean	Syn. mean	Emp. SD	Syn. SD	n_ emp	n_ syn
0	AGE_2020	0.020	0.625	0.888	0.581	61.32	61.78	24.37	24.53	3902	2100
0	HOUSESIZE	0.014	0.950	0.880	0.523	135.86	136.07	29.95	29.71	3902	2100
0	LOTSIZE	0.018	0.757	9.775	4.914	237.34	238.51	141.32	133.57	3902	2100
0	LN_DIST_CBD	0.013	0.971	0.011	0.006	7.77	7.78	0.44	0.42	3902	2100
0	LN_DIST_MEUSE	0.018	0.768	0.039	0.022	7.43	7.44	0.62	0.57	3902	2100
0	LOG_PRICE	0.115	<0.001	0.087	0.076	12.60	12.60	0.32	0.23	3902	2100
1	AGE_2020	0.018	0.993	0.948	0.650	66.84	66.25	29.31	29.10	1211	900
1	HOUSESIZE	0.035	0.535	3.453	2.150	132.16	130.07	30.90	29.32	1211	900
1	LOTSIZE	0.041	0.328	11.599	7.920	228.24	221.70	144.74	132.86	1211	900
1	LN_DIST_CBD	0.025	0.884	0.030	0.013	7.64	7.65	0.36	0.35	1211	900
1	LN_DIST_MEUSE	0.025	0.900	0.047	0.022	6.33	6.35	0.81	0.77	1211	900
1	LOG_PRICE	0.111	<0.001	0.093	0.072	12.51	12.49	0.31	0.21	1211	900

Notes: K-S D is the two-sample Kolmogorov–Smirnov distance. Quantile_RMSE (Q_RMSE) and Quantile_MAE (Q_MAE) are computed between empirical and synthetic quantiles over the 1st–99th percentiles. LOG_PRICE refers to log(Price, 2020 €). For K-S *p*-values equal to numerical underflow, we report $p < 0.001$.

Table A.2
Stratified dependence validation (Spearman correlation matrix similarity).

FP_PROTECTED	Corr_RMSE	Corr_MAE	n_pairs
0	0.0650	0.0497	15
1	0.0848	0.0684	15

Notes: Corr_RMSE and Corr_MAE summarize the discrepancy between empirical and synthetic Spearman correlation matrices using the upper triangle (excluding the diagonal). With 6 variables, the number of unique correlation pairs is 15.

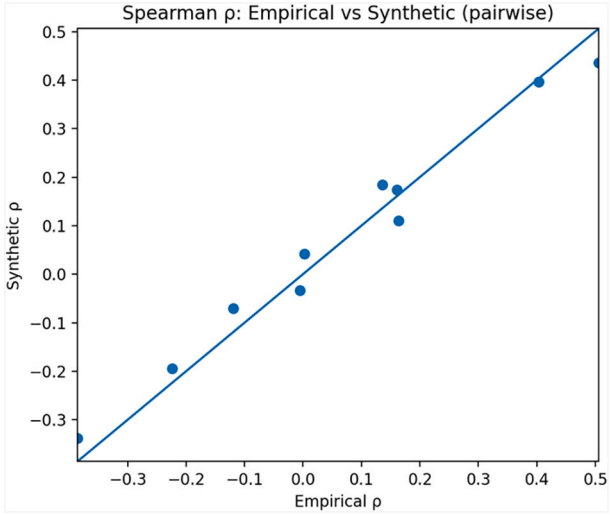

Fig. A.3. Spearman rank correlations: empirical vs. synthetic housing stock, pairwise across core variables; points near the 45° line indicate preserved associations.

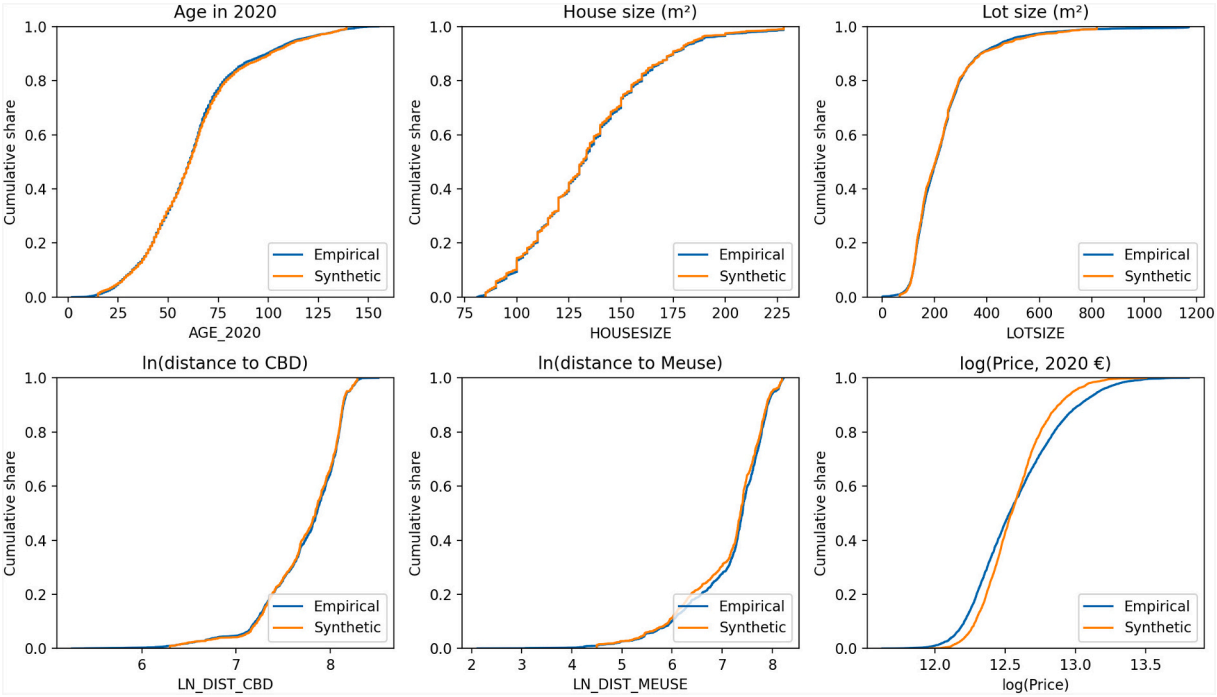

Fig. A.4. Cumulative distribution function overlays (empirical vs. synthetic) for key continues variables: age, housesize, lotsize, ln(dist_CBD), ln(dist_Meuse) -river-, log(Price).

A.3. Calibration of nature-based solutions parameters related to household decisions

Appendix A.3 describes how the amenity valuation parameters for nature-based solutions (NbS) are calibrated using empirical evidence from the hedonic pricing literature and implemented in the RHEA-NL. For clarity, Table A.3 provides an overview of the notation used in this appendix.

Table A.3
Notation for NbS amenity calibration and implementation.

Symbol	Description
i	Household index
j	Property index
r	Distance ring index (100-m empirical bins, $r = 1, \ldots, 26$)
WTP_r	Average marginal willingness to pay for NbS in distance ring r (in decimal)
d_r	Midpoint distance of distance ring r (in meters)
d_j	Exact distance from property j to the river (i.e., NbS) (in meters)
A_{ij}	NbS amenity premium perceived by household i for property j
α_{NbS}	Maximum NbS amenity premium
β_{NbS}	Spatial decay rate of NbS amenity
η_i	Household-specific NbS taste parameter
σ_η	Standard deviation of lognormal distribution for η_i

A.3.1. Empirical calibration of preferences for source urban NbS captured in housing prices

The NbS amenity parameters are calibrated based on the meta-analysis by Bockarjova et al. (2020), which synthesizes hedonic estimates of property price effects associated with different types of urban green and blue interventions. The study reports distance-specific marginal willingness-to-pay (WTP) estimates for several NbS categories, expressed as percentage changes in property prices.

To ensure conceptual alignment with the Dutch flood-adaptation context, we focus on **NbS type 4** and **NbS type 10** reported in that study, which correspond to **river and canal restoration projects**. These inverventions are the closest analogues to large-scale Dutch interventions such as *Room for the River* and the *Grensmaas* project.

The corresponding author, Marija Bockarjova, was contacted directly and kindly provided the underlying distance-specific marginal willingness-to-pay estimates for NbS types 4 and 10. These data are reported as percentage changes in property prices associated with moving 100 m closer to the NbS site. For the present study, we take the **unweighted average of NbS4 and NbS10** at each distance band to obtain a single empirical distance–WTP profile representative of river-based NbS interventions.

A.3.2. Continuous amenity specification and OLS calibration

The empirical data consist of 26 marginal WTP effects, corresponding to 100 m distance rings from 0 to 2600 m. Let $r = 1, \ldots, 26$ index these distance rings. For each ring r, WTP_r denotes the averaged marginal willingness to pay (converted to decimal form), and d_r denotes the midpoint distance (in meters).

To embed these empirical findings in the RHEA-NL, we approximate the distance–WTP relationship using an exponential decay function:

$$\mu(d) = \alpha_{\text{NbS}}.e^{-\beta_{\text{NbS}}d}, \tag{A1}$$

where a_{nbs} is the maximum amenity premium at $d = 0$, β_{NbS} controls spatial decay rate.

The parameters α_{NbS} and β_{NbS} are estimated via **ordinary least squares (OLS)** using the log-linear specification:

$$ln(WTP)_r = ln(\alpha_{\text{NbS}}) - \beta_{\text{NbS}}d_r + \varepsilon_r, \tag{A2}$$

where ε_r is an error term capturing deviations between the empirical ring mean and the fitted curve.

The OLS estimation yields:

$$\widehat{\alpha}_{\text{NbS}} \approx 0.0207, \widehat{\beta}_{\text{NbS}} \approx 0.00153,$$

with a high goodness-of-fit ($R^2 = 0.956$), indicating that the exponential decay function closely reproduces the empirical distance profile. Fig. A.5 plots the empirical marginal WTP estimates together with the fitted exponential decay curve implied by the OLS estimates.

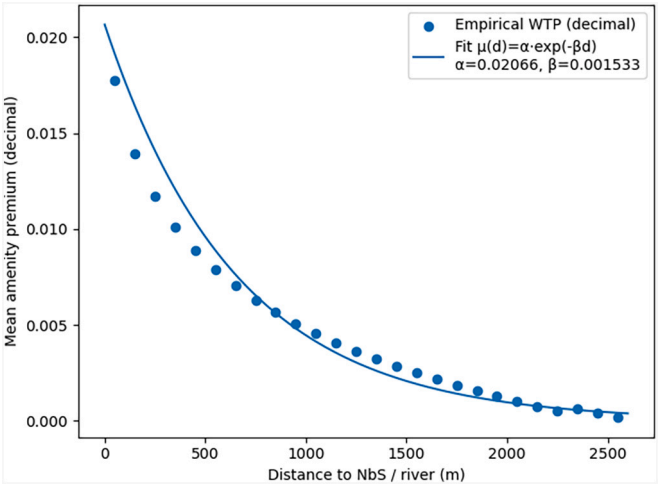

Fig. A.5. Empirical WTP from Bockarjova et al. (2020) and fitted exponential decay curve.

A.3.3. Household-level heterogeneity regarding NbS preferences

While the OLS-estimated decay function captures the **average capitalization effect**, households are likely to differ in how strongly they value NbS amenities. To represent this heterogeneity, we introduce a household-specific multiplicative taste parameter η_i, such that the amenity premium perceived by household i for property j is given by:

$$A_{ij} = \alpha_{\text{NbS}}.\eta_i.e^{-\beta_{\text{NbS}}d_j}, \tag{A3}$$

where d_j denotes the exact distance of property $j$to the river.

The parameter η_i is drawn from a lognormal distribution with mean one, ensuring that the expected amenity premium across households coincides with the empirically calibrated mean curve. The dispersion of η_i is calibrated using the coefficient of variation (CV) implied by grouped versions of the empirical distance bands. Aggregating the original 26 distance rings into five broader distance groups yields CV values ranging between approximately 0.2 and 0.5, with a median around 0.25. Mapping this dispersion to a lognormal distribution implies a standard deviation of:

$$\sigma_\eta \approx 0.25.$$

This choice introduces realistic preference heterogeneity while remaining tightly anchored to the empirical evidence. Fig. A.6 illustrates the implied distribution of η_i and the resulting dispersion of NbS amenity premiums around the mean decay curve.

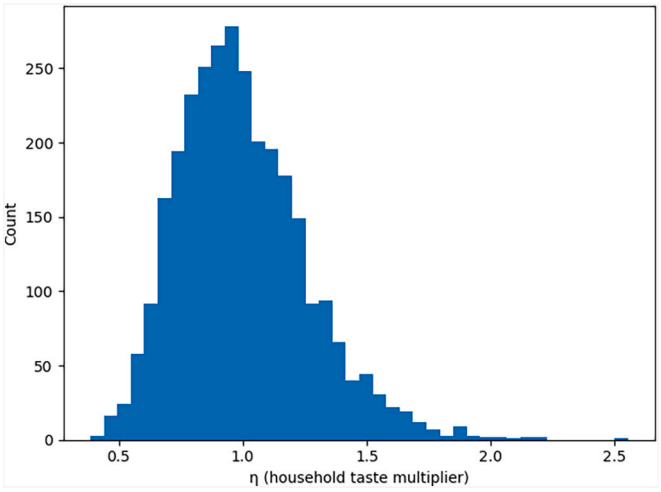

Fig. A.6. Distribution of household NbS taste multiplier η (lognormal, mean = 1).

A.3.4. Parameter variation in global sensitivity analysis

To assess robustness to uncertainty in NbS valuation in our model, we apply the global sensitivity analysis by varying the following parameters around their empirically-calibrated values:

- α_{NbS}, controlling the overall scale of the amenity premium,
- β_{NbS}, governing the spatial decay of NbS benefits,
- σ_{η}, determining the strength of household-level preference heterogeneity.

Appendix B reports technical details and results of the global sensitivity analysis. All parameters are varied within strictly positive, empirically plausible bounds, preserving the monotonic distance-decay structure and economic interpretability of NbS amenities. The results indicate that variation in NbS-related parameters primarily affects price-related outcomes, while aggregate income measures remain comparatively less sensitive. In particular, uncertainty in the magnitude and spatial decay of NbS amenities influences mean prices and price differentials without overturning the dominant role of demand pressure and endogenous trading dynamics in shaping overall market outcomes.

A.4. Results of the hedonic regression of the empirical transaction data

In Table A.4, we present the results of a hedonic price analysis on 5113 historical empirical transactions in Maastricht (1995–2020). Across specifications, properties in flood-prone dike-ring areas sell, on average, at a discount of **7–12%** relative to otherwise comparable houses. This gap should not be interpreted as the pure capitalization of flood risk: it may also reflect differences in housing stock composition (e.g., a higher share of social housing), land-use characteristics, or temporary disturbances related to the Room for the River program. Consistent with prior Dutch studies, we interpret this as **partial and incomplete capitalization** of flood risk. This motivates our agent-based simulations, where we test how demand pressure, biased risk perception, and institutional trust shape the extent to which risk is (under)valued in the market.

Table A.4
Hedonic regression results for empirical housing transactions in Maastricht (1995–2020).

	(1)	(2)	(3)	(4)
Dep. Var.: Log (Price)	Baseline OLS	PC4 FE	SEM	SAR
FP_PROTECTED	−0.118***	−0.127***	−0.090***	−0.071***
	(0.009)	(0.012)	(0.017)	(0.007)
LN_DIST_MEUSE	−0.035***	−0.043***	−0.042***	−0.027***
	(0.006)	(0.009)	(0.011)	(0.004)
LN_DIST_CBD	−0.196***	−0.199***	−0.175***	−0.134***
	(0.009)	(0.020)	(0.021)	(0.008)
HOUSESIZE	0.005***	0.004***	0.003***	0.004***
	(0.000)	(0.000)	0.000)	(0.000)
LOTSIZE	0.001***	0.001***	0.001***	0.001***
	(0.000)	(0.000)	(0.000)	(0.000)
ROOMS	0.006***	0.004**	0.004**	0.004**
	(0.002)	(0.001)	(0.001)	(0.001)
AGE	−0.002***	−0.002***	−0.001***	−0.001***
	(0.000)	(0.000)	(0.000)	(0.000)
QUALITY	0.138***	0.136***	0.127***	0.130***
	(0.006)	(0.005)	(0.005)	(0.005)
Observations	5113	5113	5113	5113
R^2	60.5	69.3		

(*continued on next page*)

Table A.4 (*continued*)

	(1)	(2)	(3)	(4)
Dep. Var.: Log (Price)	Baseline OLS	PC4 FE	SEM	SAR
Adjusted R^2	60.3	69.0		
λ (SEM)			0.732	
ρ (SAR)				0.334

Note: FP_PROTECTED is an indicator for properties located in protected flood-prone areas, shown in purple in Fig. A1.b and Fig. A2.b. PC4 FE refers to postcode fixed effects at the 4-digit level. SEM = spatial error model; SAR = spatial autoregressive model. Robust standard errors in parentheses. *** $p < 0.01$, ** $p < 0.05$, * $p < 0.1$.

A.5. Statistical comparison of the simulated transaction prices across scenarios

To formally assess whether the simulated housing market outcomes differ across our model scenarios, we apply non-parametric statistical tests to **run-level average transaction prices** in flood-prone zones at the final simulation year ($T = 30$). For each scenario, one observation per run is constructed by averaging transaction prices across all flood-prone properties within that run.

A Kruskal–Wallis rank-sum test strongly rejects the null hypothesis that all scenario outcomes are drawn from the same distribution ($p < 0.001$). Pairwise differences are then evaluated using Mann–Whitney *U* tests with Bonferroni correction for multiple comparisons ($\alpha = 0.05 / 15 \approx 0.0033$).

As shown in Table A.5, all pairwise scenario comparisons are statistically significant ($p < 0.001$), indicating that each modeled mechanism—demand pressure, behavioral risk perception, and public protection—produces a distinct distribution of market-level outcomes.

Table A.5
Pairwise Mann–Whitney *U* tests for final-year transaction prices.

Comparison	U-statistic	p-value	Significant ($\alpha = 0.0033$)
S1a vs S1b	0.0	< 0.001	Yes
S1a vs S1c	0.0	< 0.001	Yes
S1a vs S1d	0.0	< 0.001	Yes
S1a vs S2	0.0	< 0.001	Yes
S1a vs S3	0.0	< 0.001	Yes
S1b vs S1c	0.0	< 0.001	Yes
S1b vs S1d	0.0	< 0.001	Yes
S1b vs S2	0.0	< 0.001	Yes
S1b vs S3	0.0	< 0.001	Yes
S1c vs S1d	0.0	< 0.001	Yes
S1c vs S2	0.0	< 0.001	Yes
S1c vs S3	0.0	< 0.001	Yes
S1d vs S2	1.0	< 0.001	Yes
S1d vs S3	0.0	< 0.001	Yes
S2 vs S3	0.0	< 0.001	Yes

A.6. Bidding behavior: OLS regression results of the simulated transactions

This appendix reports the full OLS regression results underlying the summary coefficients discussed in Section 4.1.3. Regressions are estimated separately for scenarios S1d, S2, and S3 using transaction-level model output, with the bidding margin defined as the difference between the submitted bid and the asking price as the dependent variable.

Table A.6
OLS regression results showing the determinants of bidding behavior.

VARIABLES (*dep.var. Bid Margin*)	(S1d)	(S2)	(S3)
Intercept	0.154***	0.171***	0.217***
	(0.004)	(0.004)	(0.004)
log(Income)	−0.015***	−0.017***	−0.020***
	(0.000)	(0.000)	(0.000)
Price/Income	0.142***	0.124***	0.093***
	(0.003)	(0.003)	(0.003)
Objective FP	0.018***	0.083***	0.064***
	(0.002)	(0.007)	(0.007)
RP Bias	−0.003***	0.000*	−0.001**
	(0.000)	(0.000)	(0.000)
Observations	11,554,117	11,652,110	11,882,600
R-squared	0.150	0.153	0.181

Note: Standard errors clustered by individual simulation run and household agent are reported in parentheses. Regressions are based on model output from 100 stochastic runs over 60 timesteps (30 years). Significance levels: *** $p < 0.01$, ** $p < 0.05$, * $p < 0.1$.

Appendix B. Global sensitivity analysis

B.1. Purpose and scope

To assess the robustness of model outcomes to parameter uncertainty, we conduct a global sensitivity analysis (GSA) using the Morris Elementary Effects method (Morris, 1991a). Unlike local sensitivity analysis, GSA evaluates the relative importance of input parameters across the full multi-dimensional parameter space, which is essential for agent-based models (ABMs) characterized by non-linear interactions and stochastic path-dependencies.

Sensitivity is evaluated for Scenario S1d (high demand, biased risk perception, no public protection), and Scenario S3 (nature-based solutions with reduced flood risk and amenity co-benefits). We focus on four key outcome variables at the final simulation year (Year 30):

1. Mean market-wide transaction price,
2. Price discount between flood-prone and safe areas,
3. Mean market-wide household income,
4. Income discount between flood-prone and safe areas,

B.2. Method: Morris elementary effects

We apply the Morris screening method with a trajectory-based design (Campolongo et al., 2007). The setup includes:

- **15 trajectories**: Providing a balance between computational cost and convergence of the sensitivity indices.
- **4 levels**: Using a discrete grid for each parameter to explore the global range.
- **Replication**: To account for the intrinsic stochasticity of the ABM, each design point was evaluated across 3 independent random seeds. The elementary effects were calculated using the mean outcome of these replicates to filter simulation noise from structural parameter influence.

For each parameter, we report two primary indices:

- μ^* **(mean absolute elementary effect):** Measures the overall influence of the parameter on the output. We use the absolute version μ^* to avoid the cancellation of effects with opposing signs, providing a more robust measure of total importance.
- σ **(standard deviation of effects):** Indicates the presence of non-linear effects or interactions with other parameters.

B.3. Parameter space and scenario coverage

Table B.1 summarizes all parameters included in the global sensitivity analysis, their default values, tested bounds, and the behavioral or structural mechanisms they represent. The parameter set covers key drivers of housing market dynamics, including demand pressure, objective flood risk, loss severity, risk perception biases, liquidity effects, and adaptive bidding behavior. Note that Scenario S2 (Traditional Defense) is not analyzed separately as its parameter space is nested within the ranges of S1d, where the objective flood risk is varied as a continuous parameter.

For Scenario S3, which introduces nature-based solutions, the sensitivity analysis is extended to include NbS-specific parameters governing the magnitude, spatial decay, and heterogeneity of environmental amenity benefits (Table B.1, *Extended Parameters (only S3)*). This extended design explicitly tests uncertainty in NbS calibration while preserving comparability with the baseline parameter set used in S1d.

Table B.1
Parameters included in the global sensitivity analysis and tested mechanisms.

Symbol (paper)	Parameter (code)	Default value	Tested bounds	Rationale for inclusion
Common Parameters (S1d and S3)				
FP^{obj}	*flood_probability_obj*	0.02	[0.003, 0.03]	Objective annual flood probability used in household valuation; range reflects uncertainty and covers the reduced risk applied in S2
–	*buyer_demand*	2.0	[1.5, 2.5]	Controls demand pressure relative to supply and drives competition, affordability loss, and income-based exclusion
L	*flood_damage*	0.17	[0.10, 0.30]	Determines severity of expected flood losses conditional on flooding
–	*flood_halflife_m*	1000	[500, 2000]	Governs how quickly perceived flood risk decays with distance to the river (spatial salience)
–	*bias_k_visibility*	1.0	[0.5, 2.0]	Scales the strength of spatial salience bias
–	*bias_k_latent*	1.0	[0.5, 2.0]	Scales the strength of latent perception bias
λ	*listing_time_discount*	0.02	[0.00, 0.05]	Controls urgency-driven price discounting through time-on-market effects
–	*failure_adjustment*	0.05	[0.00, 0.08]	Captures adaptive bidding following failed transactions
Extended Parameters (only S3)				
α_{NbS}	*alpha_nbs*	0.02	[0.01, 0.03]	Controls the maximum environmental amenity premium generated by NbS
β_{NbS}	*beta_nbs*	0.0015	[0.001, 0.0025]	Governs how NbS amenity benefits decay with distance
σ_{NbS}	*sigma_nbs*	0.25	[0.15, 0.40]	Captures heterogeneity in household valuation of NbS amenities

B.4. Results

The results of the Morris global sensitivity analysis for Scenario S1d and Scenario S3 are summarized in Table B.2 and Table B.3, respectively.

B.4.1. Scenario S1d

For market-wide price and income levels, *buyer_demand* exhibits the largest μ* values, indicating that aggregate outcomes are most sensitive to variation in demand pressure. In contrast, relative outcomes comparing flood-prone and safe areas show higher sensitivity to parameters directly related to flood risk and its perception, including ***flood_probability_obj***, *flood_damage*, ***flood_halflife_m***, ***bias_k_visibility***, and ***bias_k_latent***. This pattern indicates that while demand pressure dominates aggregate market levels, spatial differentials are more sensitive to how flood risk is represented and perceived.

In addition, two behavioral adjustment parameters (***listing_time_discount*** and ***failure_adjustment***) exhibit relatively high μ* values for price-related outcomes. This reflects their direct role in the bilateral trading process: ***listing_time_discount*** affects sellers' asking prices through time-on-market adjustments, while ***failure_adjustment*** influences buyers' bidding behavior following unsuccessful purchase attempts. Their prominence in the sensitivity analysis indicates that aggregate prices are also sensitive to endogenous market-clearing mechanisms embedded in the model.

Standard deviations (σ) are moderate to high for several parameters, particularly ***listing_time_discount***, ***failure_adjustment***, and ***bias_k_latent***, suggesting the presence of nonlinearities and interaction effects in the price formation process.

Table B.2
Morris sensitivity indices for Scenario S1d (Year 30 outcomes). The values are reported as μ* (σ).

Parameter	Mean Market-Wide Price	Price discount (Flood-Prone vs. Safe)	Mean Market-Wide Income	Income discount (Flood-Prone vs. Safe)
buyer_demand	58,754 (8732)	1.53 (1.23)	9854 (1473)	2.40 (1.37)
flood_probability_obj	7814 (9973)	9.44 (7.77)	1194 (1691)	9.71 (5.87)
flood_damage	9733 (7975)	5.70 (9.03)	1459 (1976)	5.21 (7.21)
flood_halflife_m	8303 (9103)	7.96 (7.37)	1228 (1377)	8.72 (6.32)
bias_k_visibility	6188 (5897)	2.81 (3.86)	1172 (1425)	3.11 (2.50)
bias_k_latent	7756 (9837)	8.04 (8.23)	1611 (2078)	7.08 (7.32)
listing_time_discount	24,926 (29,595)	2.30 (2.57)	3943 (1426)	3.09 (3.26)
failure_adjustment	31,640 (18,390)	6.64 (7.10)	5833 (1640)	2.65 (3.99)

B.4.2. Scenario S3

Table B.3 reports Morris sensitivity indices for Scenario S3 using the extended parameter set that includes NbS-specific parameters (***alpha_nbs***, ***beta_nbs***, and ***sigma_nbs***).

As in Scenario S1d, ***buyer_demand*** remains the parameter with the highest μ* for market-wide price and income levels, indicating that aggregate outcomes remain most sensitive to demand pressure. Parameters related to flood risk and its spatial representation, particularly ***flood_probability_obj*** and ***flood_halflife_m***, continue to exhibit substantial sensitivity for relative price and income outcomes.

The NbS-specific parameters show higher μ* values for price-related outcomes than for income-related outcomes. In particular, ***alpha_nbs*** and ***beta_nbs*** display substantial μ* values for mean prices and price differentials, while their μ* values for income-related outcomes are smaller in magnitude. This indicates that, within the tested parameter ranges, housing prices are more sensitive to variation in NbS calibration than income composition measures.

Behavioral adjustment parameters (***listing_time_discount*** and ***failure_adjustment***) again exhibit relatively high μ* values for price-related outcomes, confirming that adaptive seller pricing and buyer bidding responses remain influential under the NbS configuration. The persistence of these effects across scenarios highlights the role of endogenous trading dynamics in shaping observed price levels.

Standard deviations (σ) for several parameters remain sizable, particularly for ***flood_halflife_m***, ***listing_time_discount***, and ***bias_k_latent***, indicating continued nonlinearities and interaction effects in the presence of NbS.

Table B.3
Morris sensitivity indices for Scenario S3 (Year 30 outcomes). The values are reported as μ* (σ).

Parameter	Mean Price (Market-Wide)	Price discount (Flood-Prone vs. Safe)	Mean Income (Market-wide)	Income discount (Flood-Prone vs. Safe)
buyer_demand	57,227 (8732)	2.01 (2.37)	10,428 (1898)	2.28 (2.45)
flood_probability_obj	14,859 (8786)	8.23 (3.88)	1057 (1160)	7.16 (4.17)
flood_damage	6043 (7399)	4.17 (3.87)	926 (1237)	4.88 (3.82)
flood_halflife_m	9305 (10,548)	9.98 (9.32)	1337 (1736)	10.35 (7.07)
bias_k_visibility	4612 (6447)	2.76 (3.12)	1189 (1539)	3.17 (3.20)
bias_k_latent	9826 (9809)	7.71 (8.98)	1283 (1674)	5.72 (6.67)
listing_time_discount	20,115 (23,250)	3.86 (3.78)	4693 (1657)	2.12 (3.98)
failure_adjustment	34,534 (13,718)	2.85 (2.84)	4835 (1689)	2.53 (2.91)
alpha_nbs	13,027 (9981)	2.62 (2.27)	920 (1309)	2.62 (2.02)
beta_nbs	9826 (9714)	1.87 (1.88)	690 (854)	2.05 (2.03)
sigma_nbs	7526 (9428)	1.04 (1.41)	871 (1086)	1.06 (1.36)

B.4.3. Robustness

Across both scenarios, the sensitivity analysis shows that demand pressure, flood-risk-related parameters, and endogenous market adjustment mechanisms consistently exhibit higher μ* values than other parameters. The inclusion of NbS-specific parameters in Scenario S3 introduces additional sources of sensitivity for price-related outcomes without overturning the overall ordering of influential parameters observed in Scenario S1d. Taken together, these results indicate that uncertainty in NbS valuation affects the magnitude of price responses but does not alter the qualitative structure of market dynamics identified in the main analysis. The dominant role of demand pressure and behavioral mechanisms therefore remains robust, reinforcing the conclusion that public adaptation strategies primarily reshape the spatial allocation of demand rather than fundamentally

transforming market-wide affordability or participation.

Appendix C. Local sensitivity analysis: flood-risk perception bias intensity

This appendix examines the sensitivity of model outcomes to uncertainty in the strength of behavioral flood-risk misperception. In the model, flood risk affects household decisions through expected flood loss, which depends on households' perceived flood probability. In scenarios with biased perception (S1c–S1d, S2, and S3), households distort objective flood probabilities through a spatial salience linked to distance from the river (S1c) and, in further configurations (S1d, S2, and S3), a *latent idiosyncratic perception bias* component. While the baseline calibration follows the behavioral structure described in the Data and Methodology section, the exact intensity of these perception distortions is not directly observable. The analysis reported here therefore evaluates whether the qualitative patterns documented in the results, especially price discounts in flood-prone zones, growth in exposed asset values, and income-based sorting, remain stable when the overall strength of perception bias is substantially weakened or strengthened. The results obtained through 30 simulation runs per scenario.

C.1. Bias intensity scaling: model formulation

To conduct the local sensitivity analysis, we introduce a scalar $\kappa > 0$ that uniformly scales the intensity of both channels biasing individual agent-specific risk perceptions in our ABM: spatial salience bias (Eq. (5) in the main text), and *latent idiosyncratic perception bias* reflecting individual reduced perceived risk in high-protection settings with strong trust in public defenses (Eq. 6 in the main text). The perceived log-odds of flooding are therefore:

$$\text{logit}\left(FP_{ij}^{\text{perc}}\right) \;=\; \text{logit}\left(FP_{ij}^{\text{obj}}\right) \;-\; \kappa\left(\gamma d_j \;+\; \phi b_i\right), \tag{C1}$$

and the perceived probability follows from the inverse-logit transformation:

$$FP_{ij}^{\text{perc}} \;=\; \sigma\left(\text{logit}\left(FP_{ij}^{\text{obj}}\right) \qquad \kappa\left(\gamma d_j + \phi b_i\right)\right). \tag{C2}$$

The baseline model corresponds to $\kappa = 1$. This appendix reports results for $\kappa \in \{0.5, 1.5\}$, representing a $\pm$ 50% change in overall bias intensity while leaving all other model processes unchanged.

C.2. Simulation design and reported outputs

For each bias intensity $\kappa \in \{0.5, 1.5\}$, we re-run the key biased scenarios (S1c, S1d, S2, S3) using 30 independent simulation runs over the 30-year simulation horizon (60 timesteps). Outputs are summarized in the same format as the main results to facilitate comparability. We report (i) final-year price levels and flood-prone price discounts, (ii) dynamics of average transaction prices over time in safe and flood-prone areas, (iii) Total Exposed Asset Value (TEAV) in flood-prone areas at the end of the simulation, and (iv) final-year household income levels and the income gap between flood-prone and safe areas.

C.3. Price outcomes under alternative bias intensities

Across both sensitivity cases, changing κ influences the magnitude of the flood-prone price discount in the expected direction. When bias intensity is reduced ($\kappa = 0.5$), flood-prone areas retain larger discounts relative to safe areas because perceived risk is closer to objective risk. When bias intensity is increased ($\kappa = 1.5$), discounts compress further as underestimation strengthens. Importantly, the relative ordering of scenario outcomes remains stable, and time paths remain smooth without reversals, indicating that the price formation patterns reported in the main results are not driven by a knife-edge calibration of perception bias intensity.

C.3.1. Reduced bias intensity ($\kappa = 0.5$)

Table C.1
Mean property prices at Year 30 across scenarios under reduced bias intensity ($\kappa = 0.5$). Values are reported market-wide and by zone (safe vs. flood-prone). The price discount reports the percentage difference between flood-prone and safe mean prices. Standard deviations are in parentheses.

Scenario	Price (€) (Market-wide)	Price (€) (Safe)	Price (€) (Flood-prone)	Price Discount (%) (Flood-prone vs. Safe)
S1c	365,069 (3661)	386,831 (4249)	315,609 (3534)	−18.4
S1d	366,588 (3075)	381,476 (3780)	331,824 (2680)	−13.0
S2	371,872 (3883)	378,246 (4117)	357,025 (3742)	−5.6
S3	378,628 (3418)	380,549 (3705)	374,229 (3498)	−1.7

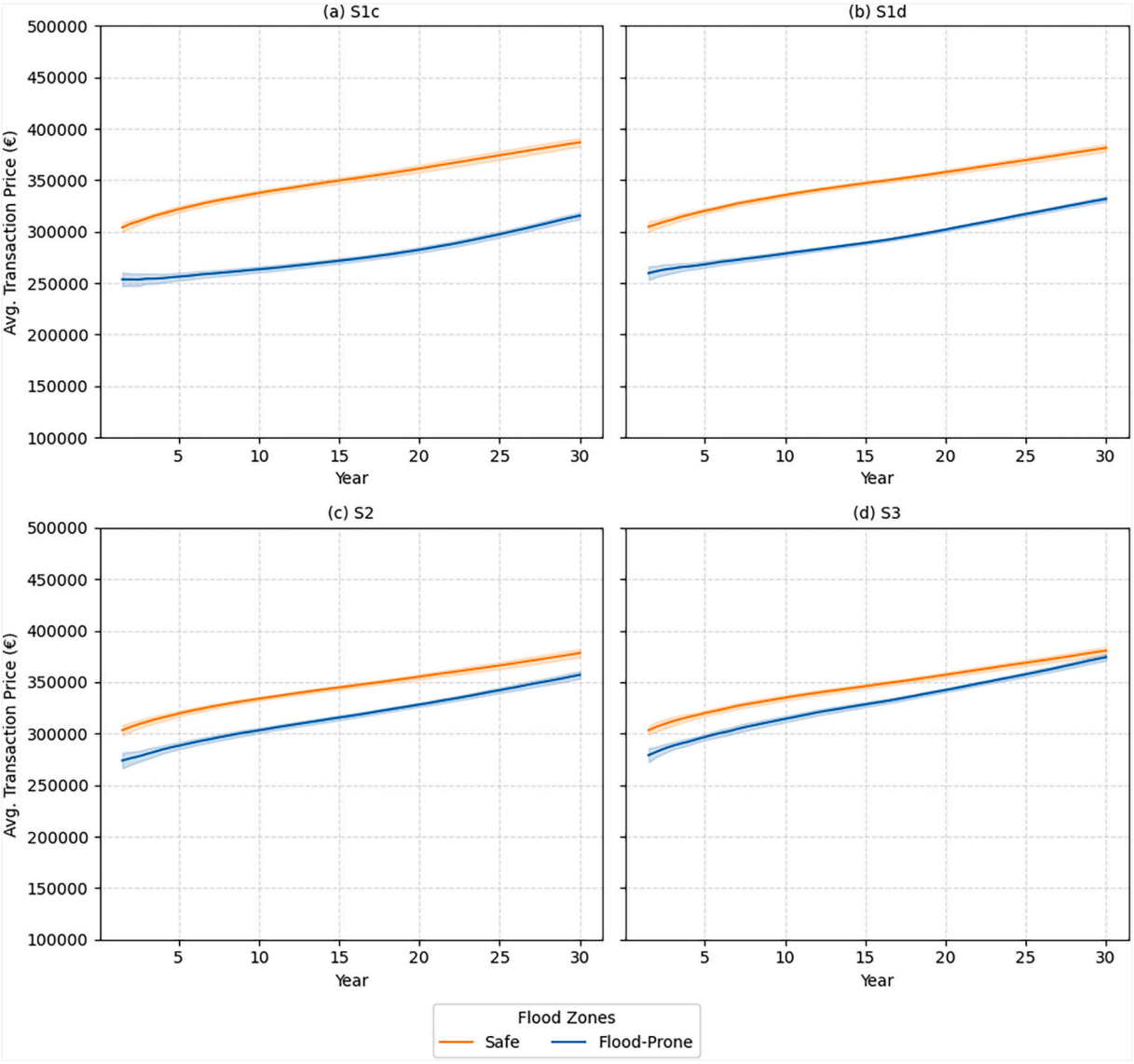

Fig. C.1. Evolution of average transaction prices across scenarios in flood-prone and safe areas over time under reduced bias intensity ($\kappa = 0.5$). Solid lines show mean prices across 30 independent simulation runs of the RHEA-NL model; shaded areas indicate the corresponding standard deviations. (a) S1c represents a high-demand market with distance-based risk discounting under an objective flood risk of 1:50, (b) S1d builds on S1c by including latent behavioral bias influencing flood risk perception. (c) S2 applies traditional flood defenses to S1d, reducing flood probability to 1:250. (d) S3 builds on S1d with nature-based solutions, which reduce flood risk to 1:250 while providing additional amenity value.

C.3.2. Increased bias intensity ($\kappa = 1.5$)

Table C.2
Mean property prices at Year 30 across scenarios under increased bias intensity ($\kappa = 1.5$). Values are reported market-wide and by zone (safe vs. flood-prone). The price discount reports the percentage difference between flood-prone and safe mean prices. Standard deviations are in parantheses.

Scenario	Price (€) (Market-wide)	Price (€) (Safe)	Price (€) (Flood-prone)	Price Discount (%) (Flood-prone vs. Safe)
S1c	367,177 (3511)	382,486 (3812)	331,720 (3501)	−13.3
S1d	370,991 (3521)	378,346 (3921)	353,822 (3090)	−6.5
S2	373,336 (2971)	377,361 (3277)	363,998 (2988)	−3.5
S3	380,400 (3400)	380,140 (3638)	381,011 (4164)	+0.2

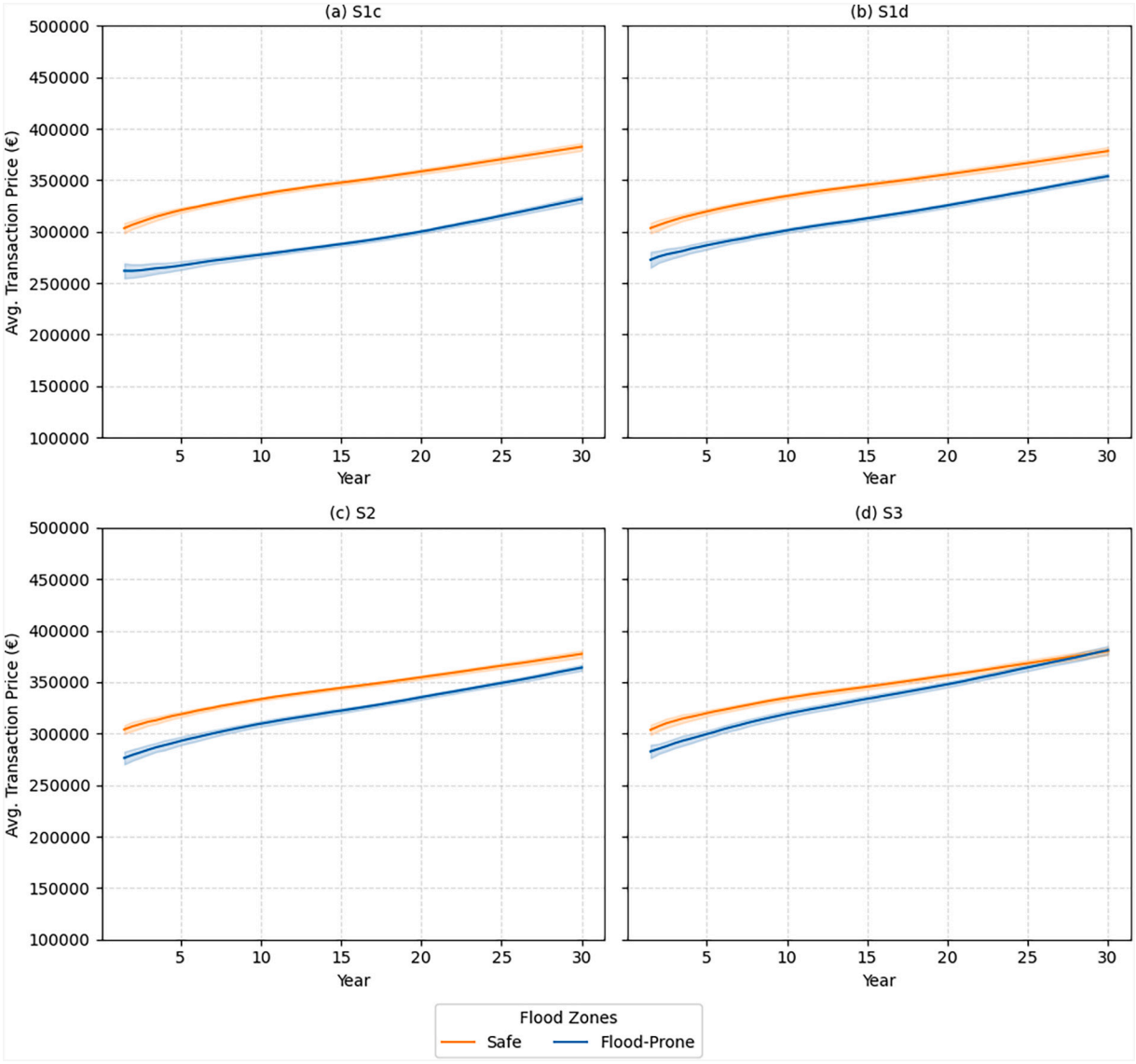

Fig. C.2. Evolution of average transaction prices across scenarios in flood-prone and safe areas over time increased bias intensity ($\kappa = 1.5$). Solid lines show mean prices across 30 independent simulation runs of the RHEA-NL model; shaded areas indicate the corresponding standard deviations. (a) S1c represents a high-demand market with distance-based risk discounting under an objective flood risk of 1:50, (b) S1d builds on S1c by including latent behavioral bias influencing flood risk perception. (c) S2 applies traditional flood defenses to S1d, reducing flood probability to 1:250. (d) S3 builds on S1d with nature-based solutions, which reduce flood risk to 1:250 while providing additional amenity value.

C.4. Exposure outcomes: TEAV

Increasing κ raises the degree to which flood-prone locations are treated as relatively attractive, which moderately increases the growth of exposed asset values. Decreasing κ dampens this mechanism. The scenario ranking and qualitative interpretation remain unchanged.

C.4.1. Reduced bias intensity ($\kappa = 0.5$)

Table C.3
Final-year exposed asset values in flood-prone areas and incremental changes across scenarios under reduced bias intensity ($\kappa = 0.5$).

Scenario	TEAV at Year 30 (€M)	Change from Year 0 (%)	Incremental Change (€M)
S1c	284.48	+15.94	–
S1d	298.74	+21.75	+14.26
S2	317.44	+29.38	+18.70
S3	329.58	+34.32	+12.14

Notes: Total Exposed Asset Value (TEAV) is measured as the aggregate value of housing assets located in flood-prone areas at the final simulation year (Year 30), reported in million euros. Values in parentheses indicate standard deviations. Percentage changes are cumulative relative to the baseline exposure in Year 0 (€245.36 million). Incremental Change reports the absolute difference in TEAV relative to the immediately preceding scenario, reflecting the marginal contribution of each sequentially introduced mechanism.

C.4.2. Increased bias intensity ($\kappa = 1.5$)

Table C.4
Final-year exposed asset values in flood-prone areas and incremental changes across scenarios under increased bias intensity ($\kappa = 1.5$).

Scenario	TEAV at Year 30 (€M)	Change from Year 0 (%)	Incremental Change (€M)
S1c	298.64	+21.71	–
S1d	315.22	+28.47	+16.58
S2	322.35	+31.38	+7.13
S3	334.43	+36.30	+12.08

Notes: Total Exposed Asset Value (TEAV) is measured as the aggregate value of housing assets located in flood-prone areas at the final simulation year (Year 30), reported in million euros. Values in parentheses indicate standard deviations. Percentage changes are cumulative relative to the baseline exposure in Year 0 (€245.36 million). Incremental Change reports the absolute difference in TEAV relative to the immediately preceding scenario, reflecting the marginal contribution of each sequentially introduced mechanism.

C.5. Income sorting outcomes under alternative bias intensities

Income differences between safe and flood-prone areas respond systematically to bias intensity. Under weaker bias ($\kappa = 0.5$), flood-prone areas remain more strongly associated with lower incomes because risk is more accurately perceived and capitalized. Under stronger bias ($\kappa = 1.5$), flood-prone zones become relatively more attractive to higher-income households, narrowing the income gap with safe zones. Market-wide mean incomes remain broadly stable across the sensitivity cases, consistent with the interpretation that bias intensity primarily affects spatial distribution of demand rather than overall market participation.

C.5.1. Reduced bias intensity ($\kappa = 0.5$)

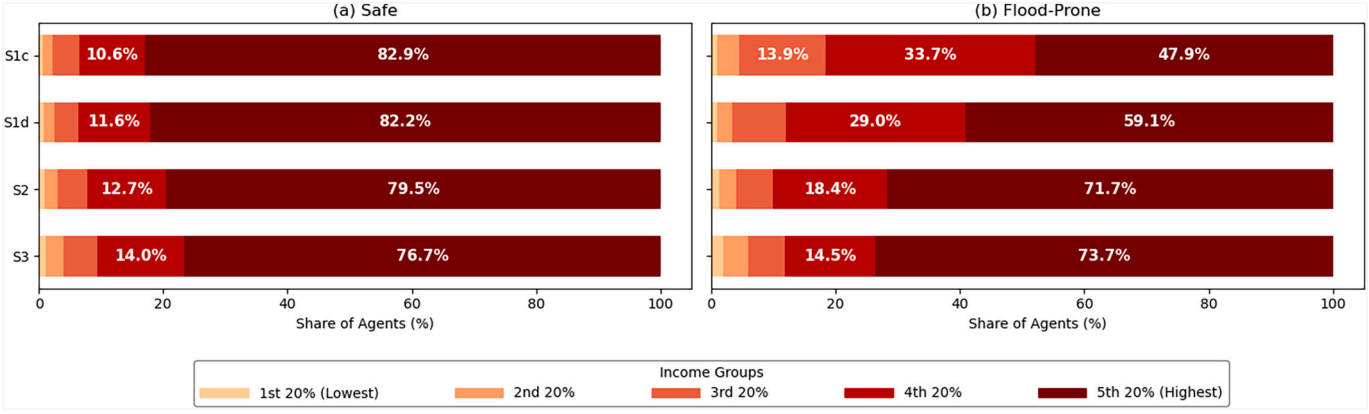

Fig. C.3. Final-year normalized income group composition in flood-prone and safe areas across scenarios under reduced bias intensity ($\kappa = 0.5$). Percentage shares above 10% are labeled directly on the bars for readability.

Table C.5
Average household incomes across scenarios in the final simulation year (Year 30) under reduced bias intensity ($\kappa = 0.5$). The means are grouped in three categories: Market-wide (combines safe and flood-prone), Safe, and Flood-prone. Income discount column shows the percentage difference between the mean income in flood-prone zones and safe (€; mean and SD).

Scenario	Income (€) (Market-wide)	Income (€) (Safe)	Income (€) (Flood-prone)	Income Discount (%) (Flood-Prone vs. Safe)
S1c	64,849 (775)	70,113 (855)	52,879 (897)	−24.6
S1d	65,339 (594)	69,273 (741)	56,152 (670)	−18.9
S2	66,374 (852)	68,174 (904)	62,181 (910)	−8.8
S3	67,018 (831)	67,567 (898)	65,763 (912)	−2.7

C.5.2. Increased bias intensity ($\kappa = 1.5$)

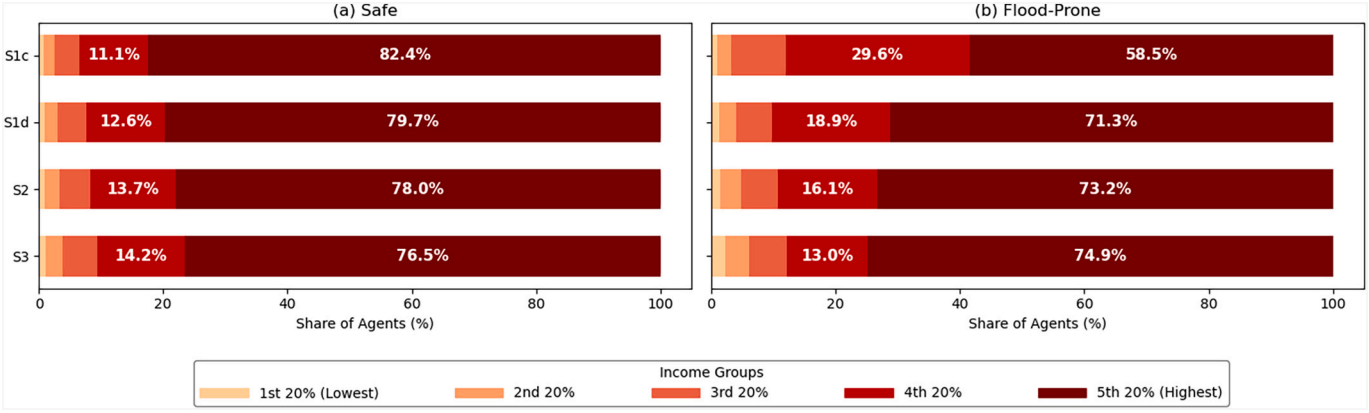

Fig. C.4. Normalized income group composition in flood-prone and safe areas across scenarios at the final simulation year (Year 30) increased bias intensity ($\kappa = 1.5$). Percentage shares above 10% are labeled directly on the bars for readability.

Table C.6
Household incomes across scenarios in the final simulation year (Year 30) under increased bias intensity ($\kappa = 1.5$). The means are grouped in three categories: Market-wide (combines safe and flood-prone), Safe, and Flood-prone. Income discount column shows the percentage difference between the mean income in flood-prone zones and safe (€; mean and SD).

Scenario	Income (€) (Market-wide)	Income (€) (Safe)	Income (€) (Flood-prone)	Income Discount (%) (Flood-Prone vs. Safe)
S1c	65,336 (711)	69,264 (736)	56,236 (832)	−18.8
S1d	66,292 (790)	68,379 (872)	61,421 (826)	−10.2
S2	66,574 (605)	67,720 (708)	63,916 (650)	−5.6
S3	67,229 (822)	67,270 (866)	67,137 (1107)	−0.2

C.6. Interpretation

Varying bias intensity by ±50% produces monotonic shifts in price discounts, exposure growth, and income gaps between safe and flood-prone areas, but these changes are quantitative rather than qualitative. The core mechanisms documented in the main results remain intact: demand pressure governs overall market tightness and affordability constraints, perception bias modifies the extent to which flood-prone locations are treated as attractive by higher-income households, and public flood defenses further reinforces price and income convergence in flood-prone areas through objective risk reduction and, in the case of nature-based solutions, additional amenity capitalization. The stability of scenario rankings and time-path patterns across the two sensitivity cases indicates that the principal conclusions are not dependent on a narrow calibration of the perception-bias intensity.

Data availability

Due to a non-disclosure agreement with NVM, the original transaction data cannot be shared. The model code and configuration for reproducibility are available on GitHub: https://github.com/SC3-TUD/CEUS_RHEA-NL (repository will be publicly accessible upon publication).

References

Aerts, J. C. J. H. (2020). Integrating agent-based approaches with flood risk models: A review and perspective. *Water Security, 11*, Article 100076. https://doi.org/10.1016/j.wasec.2020.100076

Aerts, J. C. J. H., Botzen, W. J. W., Emanuel, K., Lin, N., De Moel, H., & Michel-Kerjan, E. O. (2014). Evaluating flood resilience strategies for coastal megacities. *Science, 344*, 473–475. https://doi.org/10.1126/science.1248222

Anguelovski, I., Connolly, J. J. T., Cole, H., Garcia-Lamarca, M., Triguero-Mas, M., Baró, F., … Minaya, J. M. (2022). Green gentrification in European and North American cities. *Nature Communications, 13*, 3816. https://doi.org/10.1038/s41467-022-31572-1

Anguelovski, I., Connolly, J. J. T., Pearsall, H., Shokry, G., Checker, M., Maantay, J., … Roberts, J. T. (2019). Why green "climate gentrification" threatens poor and vulnerable populations. *Proceedings. National Academy of Sciences. United States of America, 116*, 26139–26143. https://doi.org/10.1073/pnas.1920490117

Arthur, W. B. (2021). Foundations of complexity economics. *Nature Reviews Physics, 3*, 136–145. https://doi.org/10.1038/s42254-020-00273-3

Axtell, R. L., & Farmer, J. D. (2025). *Agent-based modeling in economics and finance: Past, present, and future*.

Baan, P. J. A., & Klijn, F. (2004). Flood risk perception and implications for flood risk management in the Netherlands. *International Journal of River Basin Management, 2*, 113–122. https://doi.org/10.1080/15715124.2004.9635226

Baldauf, M., Garlappi, L., & Yannelis, C. (2020). Does climate change affect real estate prices? Only if you believe in it. *The Review of Financial Studies, 33*, 1256–1295. https://doi.org/10.1093/rfs/hhz073

Bank of England. (2021). *Key elements of the 2021 biennial exploratory scenario: Financial risks from climate change*. Bank of England.

Bernstein, A., Gustafson, M. T., & Lewis, R. (2019). Disaster on the horizon: The price effect of sea level rise. *Journal of Financial Economics, 134*, 253–272. https://doi.org/10.1016/j.jfineco.2019.03.013

Bockarjova, M., Botzen, W. J. W., van Schie, M. H., & Koetse, M. J. (2020). Property price effects of green interventions in cities: A meta-analysis and implications for gentrification. *Environmental Science & Policy, 112*, 293–304. https://doi.org/10.1016/j.envsci.2020.06.024

Botzen, W. J. W., Aerts, J. C. J. H., & van den Bergh, J. C. J. M. (2009a). Dependence of flood risk perceptions on socio-economic and objective risk factors: Individual perceptions of climate change. *Water Resources Research, 45*. https://doi.org/10.1029/2009WR007743

Botzen, W. J. W., Aerts, J. C. J. H., & Van Den Bergh, J. C. J. M. (2009b). Dependence of flood risk perceptions on socio-economic and objective risk factors. *Water Resources Research, 45*, Article 2009WR007743. https://doi.org/10.1029/2009WR007743

Brander, L. M., & Koetse, M. J. (2011). The value of urban open space: Meta-analyses of contingent valuation and hedonic pricing results. *Journal of Environmental Management, 92*, 2763–2773. https://doi.org/10.1016/j.jenvman.2011.06.019

Bubeck, P., Botzen, W. J. W., & Aerts, J. C. J. H. (2012). A review of risk perceptions and other factors that influence flood mitigation behavior: Review of flood risk

perceptions. *Risk Analysis, 32*, 1481–1495. https://doi.org/10.1111/j.1539-6924.2011.01783.x
Burningham, K., Fielding, J., & Thrush, D. (2008). 'Itll never happen to me': Understanding public awareness of local flood risk. *Disasters, 32*, 216–238. https://doi.org/10.1111/j.1467-7717.2007.01036.x
Campolongo, F., Cariboni, J., & Saltelli, A. (2007). An effective screening design for sensitivity analysis of large models. *Environmental Modelling & Software, 22*, 1509–1518. https://doi.org/10.1016/j.envsoft.2006.10.004
Collenteur, R. A., De Moel, H., Jongman, B., & Di Baldassarre, G. (2015). The failed-levee effect: Do societies learn from flood disasters? *Natural Hazards, 76*, 373–388. https://doi.org/10.1007/s11069-014-1496-6
Crooks, A., Heppenstall, A., Manley, E., Malleson, N., 2018. Agent-based modelling and geographical information systems: A practical primer.
Di Baldassarre, G., Kreibich, H., Vorogushyn, S., Aerts, J., Arnbjerg-Nielsen, K., Barendrecht, M., … Ward, P. J. (2018). Hess opinions: An interdisciplinary research agenda to explore the unintended consequences of structural flood protection. *Hydrology and Earth System Sciences, 22*, 5629–5637. https://doi.org/10.5194/hess-22-5629-2018
Di Baldassarre, G., Viglione, A., Carr, G., Kuil, L., Yan, K., Brandimarte, L., & Blöschl, G. (2015). Debates—Perspectives on socio-hydrology: Capturing feedbacks between physical and social processes. *Water Resources Research, 51*, 4770–4781. https://doi.org/10.1002/2014WR016416
Endendijk, T., Botzen, W.J.W., de Moel, H., Kok, M., 2023. Experience from the 2021 Floods in the Netherlands: Household Survey Results on Impacts and Responses 2.
Engbersen, D., Biesbroek, R., & Termeer, C. J. A. M. (2024). Between theory and action: Assessing the transformative character of climate change adaptation in 51 cases in the Netherlands. *Global Environmental Change, 89*, Article 102948. https://doi.org/10.1016/j.gloenvcha.2024.102948
Ettema, D. (2011). A multi-agent model of urban processes: Modelling relocation processes and price setting in housing markets. *Computers, Environment and Urban Systems, 35*, 1–11. https://doi.org/10.1016/j.compenvurbsys.2010.06.005
Filatova, T., Parker, D. C., & Van Der Veen, A. (2011). The implications of skewed risk perception for a Dutch coastal land market: Insights from an agent-based computational economics model. *Journal of Agricultural and Resource Economics, 40*, 405–423. https://doi.org/10.1017/S1068280500002860
Filatova, T. (2015). Empirical agent-based land market: Integrating adaptive economic behavior in urban land-use models. *Computers, Environment and Urban Systems, 54*, 397–413. https://doi.org/10.1016/j.compenvurbsys.2014.06.007
Frantzeskaki, N. (2019). Seven lessons for planning nature-based solutions in cities. *Environmental Science & Policy, 93*, 101–111. https://doi.org/10.1016/j.envsci.2018.12.033
Ge, J. (2017). Endogenous rise and collapse of housing price. *Computers, Environment and Urban Systems, 62*, 182–198. https://doi.org/10.1016/j.compenvurbsys.2016.11.005
van Ginkel, K., Rijken, B., Hoogvliet, M., van Veggel, W., Botzen, W., Filatova, T., 2025. How an economic and financial perspective could guide transformational adaptation to sea level rise. SSRN.
Glaeser, E., & Gyourko, J. (2018). The economic implications of housing supply. *Journal of Economic Perspectives, 32*, 3–30. https://doi.org/10.1257/jep.32.1.3
Gourevitch, J. D., Kousky, C., Liao, Y., Nolte, C., Pollack, A. B., Porter, J. R., & Weill, J. A. (2023). Unpriced climate risk and the potential consequences of overvaluation in U. S. housing markets. *Nature Climate Change, 13*, 250–257. https://doi.org/10.1038/s41558-023-01594-8
Groot, C., & Groot, S. (2024). *Housing market quarterly report: House price rise increases.* RaboResearch.
Guerrero, O. A. (2020). Decentralized markets and the emergence of housing wealth inequality. *Computers, Environment and Urban Systems, 84*, Article 101541. https://doi.org/10.1016/j.compenvurbsys.2020.101541
Guerrieri, V., Hartley, D., & Hurst, E. (2013). Endogenous gentrification and housing price dynamics. *Journal of Public Economics, 100*, 45–60. https://doi.org/10.1016/j.jpubeco.2013.02.001
Haer, T., Husby, T. G., Botzen, W. J. W., & Aerts, J. C. J. H. (2020). The safe development paradox: An agent-based model for flood risk under climate change in the European union. *Global Environmental Change, 60*, Article 102009. https://doi.org/10.1016/j.gloenvcha.2019.102009
Hallegatte, S., Green, C., Nicholls, R. J., & Corfee-Morlot, J. (2013). Future flood losses in major coastal cities. *Nature Climate Change, 3*, 802–806. https://doi.org/10.1038/nclimate1979
van Herk, S., Rijke, J., Zevenbergen, C., Ashley, R., & Besseling, B. (2015). Adaptive co-management and network learning in the room for the river programme. *Journal of Environmental Planning and Management, 58*, 554–575. https://doi.org/10.1080/09640568.2013.873364
IPCC. (2022). *Climate change 2022 – Impacts, adaptation and vulnerability: Working group II contribution to the sixth assessment report of the intergovernmental panel on climate change* (1st ed.). Cambridge University Press. https://doi.org/10.1017/9781009325844
Kahneman, D., & Tversky, A. (1979). Prospect theory: An analysis of decision under risk. *Econometrica, 47*, 263. https://doi.org/10.2307/1914185
de Koning, K., & Filatova, T. (2020). Repetitive floods intensify outmigration and climate gentrification in coastal cities. *Environmental Research Letters, 15*, Article 034008. https://doi.org/10.1088/1748-9326/ab6668
Kousky, C. (2010). Learning from extreme events: Risk perceptions after the flood. *Land Economics, 86*, 395–422. https://doi.org/10.3368/le.86.3.395
Lechowska, E. (2018). What determines flood risk perception? A review of factors of flood risk perception and relations between its basic elements. *Natural Hazards, 94*, 1341–1366. https://doi.org/10.1007/s11069-018-3480-z
Magliocca, N., Safirova, E., McConnell, V., & Walls, M. (2011). An economic agent-based model of coupled housing and land markets (CHALMS). *Computers, Environment and Urban Systems, 35*, 183–191. https://doi.org/10.1016/j.compenvurbsys.2011.01.002
Magliocca, N. R., & Walls, M. (2018). The role of subjective risk perceptions in shaping coastal development dynamics. *Computers, Environment and Urban Systems, 71*, 1–13. https://doi.org/10.1016/j.compenvurbsys.2018.03.009
Mol, J. M., Botzen, W. J. W., Blasch, J. E., & Moel, H. (2020). Insights into flood risk misperceptions of homeowners in the Dutch river delta. *Risk Analysis, 40*, 1450–1468. https://doi.org/10.1111/risa.13479
Morris, M.D., 1991. Factorial sampling plans for preliminary computational experiments 33(2), 161–174.
Mutlu, A., Roy, D., & Filatova, T. (2023). Capitalized value of evolving flood risks discount and nature-based solution premiums on property prices. *Ecological Economics, 205*, 107682. https://doi.org/10.1016/j.ecolecon.2022.10768
Nesshöver, C., Assmuth, T., Irvine, K. N., Rusch, G. M., Waylen, K. A., Delbaere, B., … Wittmer, H. (2017). The science, policy and practice of nature-based solutions: An interdisciplinary perspective. *Science of the Total Environment, 579*, 1215–1227. https://doi.org/10.1016/j.scitotenv.2016.11.106
OECD Environment Policy Papers. (2020). *Nature-based solutions for adapting to water-related climate risks (OECD environment policy papers no. 21)*. OECD Environment Policy Papers. https://doi.org/10.1787/2257873d-en
O'Neill, E., Brereton, F., Shahumyan, H., & Clinch, J. P. (2016). The impact of perceived flood exposure on flood-risk perception: The role of distance. *Risk Analysis, 36*, 2158–2186. https://doi.org/10.1111/risa.12597
O'Sullivan, D., Evans, T., Manson, S., Metcalf, S., Ligmann-Zielinska, A., & Bone, C. (2016). Strategic directions for agent-based modeling: Avoiding the YAAWN syndrome. *Journal of Land Use Science, 11*, 177–187. https://doi.org/10.1080/1747423X.2015.1030463
Parker, D. C., & Filatova, T. (2008). A conceptual design for a bilateral agent-based land market with heterogeneous economic agents. *Computers, Environment and Urban Systems, 32*, 454–463. https://doi.org/10.1016/j.compenvurbsys.2008.09.012
Pryce, G., Chen, Y., & Galster, G. (2011). The impact of floods on house prices: An imperfect information approach with myopia and amnesia. *Housing Studies, 26*, 259–279. https://doi.org/10.1080/02673037.2011.542086
van Reeken, J., & Phlippen, S. (2022). *Is flood risk already affecting house prices? Lessons learned from an impact assessment study in the Netherlands.* ABN AMRO Bank N.V.
Rice, J. L., Cohen, D. A., Long, J., & Jurjevich, J. R. (2020). Contradictions of the climate-friendly city: New perspectives on eco-gentrification and housing justice. *International Journal of Urban and Regional Research, 44*, 145–165. https://doi.org/10.1111/1468-2427.12740
Robinson, P. J., & Botzen, W. J. W. (2019). Determinants of probability neglect and risk attitudes for disaster risk: An online experimental study of flood insurance demand among homeowners. *Risk Analysis, 39*, 2514–2527. https://doi.org/10.1111/risa.13361
Seddon, N., Chausson, A., Berry, P., Girardin, C. A. J., Smith, A., & Turner, B. (2020). Understanding the value and limits of nature-based solutions to climate change and other global challenges. *Philosophical Transactions of the Royal Society B, 375*, Article 20190120. https://doi.org/10.1098/rstb.2019.0120
Sirenko, M., Filatova, T., 2025. It's not just risk—it's responsibility: Changing drivers of home flood protection. Accepted Manuscript. doi:10.31223/X51J1M.
Taberna, A., Filatova, T., Roy, D., & Noll, B. (2020). Tracing resilience, social dynamics and behavioral change: A review of agent-based flood risk models. *SESMO, 2*, Article 17938. https://doi.org/10.18174/sesmo.2020a17938
Taylor, Z. J., & Aalbers, M. B. (2022). Climate gentrification: Risk, rent, and restructuring in greater Miami. *Annals of the American Association of Geographers, 112*, 1685–1701. https://doi.org/10.1080/24694452.2021.2000358
Terpstra, T. (2011). Emotions, trust, and perceived risk: Affective and cognitive routes to flood preparedness behavior: Affective and cognitive routes to flood preparedness behavior. *Risk Analysis, 31*, 1658–1675. https://doi.org/10.1111/j.1539-6924.2011.01616.x
Tobin, G. A. (1995). The levee love affair: A stormy relationship? *J American Water Resour Assoc, 31*, 359–367. https://doi.org/10.1111/j.1752-1688.1995.tb04025.x
UNDRR, & CRED. (2020). *The human cost of disasters: An overview of the last 20 years (2000–2019)*. Geneva, Switzerland: United Nations Office for Disaster Risk Reduction (UNDRR) and Centre for Research on the Epidemiology of Disasters (CRED).
UN-Habitat. (2024). *World cities report 2024: Cities and climate action.* United Nations Human Settlements Programme.
Votsis, A. (2017). Planning for green infrastructure: The spatial effects of parks, forests, and fields on Helsinkis apartment prices. *Ecological Economics, 132*, 279–289. https://doi.org/10.1016/j.ecolecon.2016.09.029
Waltert, F., & Schläpfer, F. (2010). Landscape amenities and local development: A review of migration, regional economic and hedonic pricing studies. *Ecological Economics, 70*, 141–152. https://doi.org/10.1016/j.ecolecon.2010.09.031
Wigt, P., Romijn, G., & van Dijk. (2012). *Moving behaviour in the Dutch owner occupied housing market.* CPB Netherlands Bureau for Economic Policy Analysis.